# Exergoeconomic and environmental analyses of $CO_2/NH_3$ cascade refrigeration systems equipped with different types of flash tank intercoolers

Mosaffa, A. H.; Farshi, L. Garousi; Infante Ferreira, C. A.; Rosen, M. A.

**DOI**
10.1016/j.enconman.2016.03.053

**Publication date**
2016

**Document Version**
Accepted author manuscript

**Published in**
Energy Conversion and Management

Formal publication: Energy Conversion and Management (Elsevier), Volume 117, 1 June 2016, pages 442-453.
Doi: http://dx.doi.org/10.1016/j.enconman.2016.03.053

## Research Highlights

- $CO_2/NH_3$ cascade refrigeration cycles with flash intercoolers are investigated.
- Exergoeconomic factors of components are determined to assess their relative significances.
- An environmental analysis is applied to determine the penalty cost of GHG emission.
- The effects of operating parameters on COP, exergy efficiency and total cost rate are investigated.
- An optimization is applied based on the maximum COP and the minimum total cost rate.

# Exergoeconomic and environmental analyses of $CO_2/NH_3$ cascade refrigeration systems equipped with different types of flash tank intercoolers

**A.H. Mosaffa[1*], L. Garousi Farshi [2], C.A. Infante Ferreira[3], M.A. Rosen[4]**

[1] *Department of Mechanical Engineering, Azarbaijan Shahid Madani University, Tabriz, Iran*

[2] *Faculty of Mechanical Engineering, University of Tabriz, Iran*

[3] *Delft University of Technology, Department Process & Energy, Delft, 2628 CB, Netherlands*

[4] *Faculty of Engineering and Applied Science, University of Ontario Institute of Technology, Oshawa, ON, L1H 7K4, Canada*

* Corresponding author. Tel.: +98 412 4327566, E-mail addresses: mosaffa@azaruniv.ac.ir

**Abstract:**

Exergoeconomic and environmental analyses are presented for two $CO_2/NH_3$ cascade refrigeration systems equipped with 1) two flash tanks, and 2) a flash tank along with a flash intercooler with indirect subcooler. A comparative study is performed for the proposed systems, and optimal values of operating parameters of the system are determined that maximize the coefficient of performance (COP) and exergy efficiency and minimize the total annual cost. The operating parameters considered include condensing temperatures of $NH_3$ in the condenser and $CO_2$ in the cascade heat exchanger, the evaporating temperature of $CO_2$ in the evaporator, the temperature difference in the cascade heat exchanger, the intermediate pressure of the flash tank in the $CO_2$ low-temperature circuit, the mass flow rate ratio in the flash intercooler and the degree of superheating of the $CO_2$ at the evaporator outlet. The total annual cost includes the capital, operating and maintenance costs and the penalty cost of GHG emission. The results show that, the total annual cost rate for system 1 is 11.2% and

11.9% lower than that for system 2 referring to thermodynamic and economic optimizations, respectively. For thermodynamic and cost optimal design condition the COP and exergy efficiency of both systems are almost the same. Finally, in order to obtain the best balance between exergy destruction cost and capital cost, the exergoeconomic factor is defined for each component of proposed systems, for cases in which the system operates at the best performance conditions.

**Keywords:** Cascade refrigeration system; $CO_2/NH_3$; Exergoeconomic analysis; Environmental analysis; Optimization; Flash tank.

**Nomenclature**

| | |
|---|---|
| $A$ | area ($m^2$) |
| $c$ | unit cost of exergy ($ $kJ^{-1}$) |
| $\dot{C}$ | cost rate ($ $s^{-1}$) |
| $CO_2e$ | carbon dioxide equivalent |
| COP | coefficient of performance |
| CRF | capital recovery factor |
| $E$ | electrical energy consumption (kWh) |
| $\dot{E}x$ | exergy rate (kW) |
| $f$ | exergoeconomic factor |
| $F$ | correction factor |
| FT | flash tank |
| FIS | flash intercooler with indirect subcooler |
| GHG | greenhouse gas |
| GWP | global warming potential |
| $h$ | specific enthalpy (kJ $kg^{-1}$) |

| | |
|---|---|
| HTC | high-temperature compressor |
| $i$ | annual interest rate |
| LTC | low-temperature compressor |
| $\dot{m}$ | mass flow rate (kg $s^{-1}$) |
| $m$ | mass (kg) |
| $n$ | system life time (year) |
| $N$ | operational hours in a year (h) |
| ODP | ozone depletion potential |
| $P$ | pressure (kPa) |
| $PR$ | pressure ratio |
| $\dot{Q}$ | heat rate (kW) |
| $r$ | mass flow rate ratio |
| $s$ | specific entropy (kJ $kg^{-1}$ $K^{-1}$) |
| $T$ | temperature (°C or K) |
| TV | throttling valve |
| $\Delta T_{lm}$ | logarithmic mean temperature difference (K) |
| $U_o$ | overall heat transfer coefficient (W $m^{-2}$ $K^{-1}$) |
| $\dot{V}$ | volumetric flow rate ($m^3$ $s^{-1}$) |
| $\dot{W}$ | electrical power (kW) |
| $\dot{Z}$ | capital cost rate ($ $s^{-1}$) |
| $Z$ | capital cost ($) |
| *Greek symbols* | |
| $\alpha_{el}$ | unit electricity cost ($ $kWh^{-1}$) |
| $\phi$ | maintenance factor |

| | |
|---|---|
| $\eta$ | energy efficiency |
| $\mu_{CO_2e}$ | emission conversion factor (kg $kWh^{-1}$) |
| $\psi$ | exergy efficiency |
| *Subscripts* | |
| 0 | ambient |
| ca | cooled air |
| CAS | cascade heat exchanger |
| CD | condenser |
| CM | compressor |
| D | destruction |
| e | exit |
| env | environment |
| el | electricity |
| EV | evaporator |
| F | fuel |
| i | inlet |
| int | intermediate |
| k | *k*th component |
| m | mechanical |
| OP | operation |
| P | product |
| s | isentropic |
| sup | superheating |
| t | thermal |

## 1. Introduction

The use of $CO_2$ as a working fluid in refrigeration cycles has expanded notably in recent years, because it has low global warming potential (GWP) and no ozone depletion potential (ODP). It is also non-flammable, inexpensive and abundant in nature. Moreover, $CO_2$ (R744) has advantages in use as a refrigerant in low temperature applications such as storage of frozen food and rapid freezing systems. Despite of these advantages of $CO_2$ as a working fluid in refrigeration cycles, using carbon dioxide as the working fluid in a single stage refrigeration cycle is normally not economical due to the high pressure difference between evaporator and condenser. In single stage refrigeration systems using $CO_2$ as a refrigerant, a high pressure ratio and condensation close to the critical conditions lead to a low coefficient of performance (COP) in comparison with the refrigeration cycles working with HFC refrigerants [1].

Two-stage compression systems and cascade refrigeration cycles can be used for these applications to overcome the aforementioned problem [2–7]. A cascade refrigeration cycle involves two refrigeration circuits which are thermally coupled through an internal cascade heat exchanger. The internal cascade heat exchanger plays the role of condenser for the low temperature circuit and evaporator for the high temperature circuit. The $CO_2/NH_3$ cascade refrigeration cycle uses two natural refrigerants, $NH_3$ (R717) in the high temperature circuit and $CO_2$ in the low temperature circuit, and is a well-known system in refrigeration industry. Research on $CO_2/NH_3$ cascade refrigeration has been reported by several authors. Lee et al. [8] thermodynamically assessed a $CO_2/NH_3$ cascade refrigeration to determine the optimal condensing temperature of the cascade heat exchanger to maximize the COP and minimize the exergy destruction of the system. Getu and Bansal [9] thermodynamically analyzed a $CO_2/NH_3$ cascade refrigeration system and optimized several cycle operating parameters: condensing, evaporating, subcooling and superheating temperatures and temperature difference in the cascade heat exchanger. They showed that an increase in subcooling before expansion to the evaporator increased the COP of the system while an increase in superheating and condensing temperature decreased the COP. Dopazo et al. [10] analyzed a $CO_2/NH_3$ cascade refrigeration system and identified the optimum $CO_2$ condensing temperature based on energy and exergy points of view. Bingming et al. [11] experimentally investigated the effects of operation parameters on the performance of a $CO_2/NH_3$ cascade refrigeration system, and showed that the system COP is greatly affected by evaporating and condensing temperatures and temperature difference in cascade heat exchanger while it is only slightly sensitive to the degree of superheating. Dopazo and Fernandez-Seara [12] experimentally evaluated a $CO_2/NH_3$ cascade refrigeration system for an industrial freezer with a –50 °C evaporating temperature. They also investigated the influence of the operating parameters on system performance and compared the results with those for common $NH_3$ two stage refrigeration systems under the same operating conditions. They concluded that the COP of the cascade system is similar to the COP of an ammonia double stage with intercooler and about 20% higher when an economizer is applied. Ma et al. [13] thermodynamically analyzed a $CO_2/NH_3$ cascade refrigeration system using a falling film evaporator–condenser as the cascade heat exchanger, and showed that the use of such a heat exchanger improved the system COP by providing a smaller temperature difference.

After a technical feasibility study, the thermodynamic analysis must be completed with considerations about the costs of systems incorporated. Therefore, an economic analysis should also be considered for analyzing a refrigeration plant. Mitishita et al. [14] developed an optimization methodology to reduce power consumption and costs for frost-free refrigerators. This methodology was used to determine the compressor size and efficiency, the number of condenser and evaporator fins and the evaporator air flow rate in order to minimize energy consumption. Various studies based on exergy and thermoeconomic concepts in relation to heat pumps [15–17] and refrigeration systems have been previously published. Rezayan and Behbahaninia [18] presented a thermoeconomic optimization for a simple $CO_2/NH_3$ cascade refrigeration system without considering environmental analysis. They investigated the influence of design parameters on total annual cost of the system when ambient temperature, cooling capacity and cold space temperature are constraints. Exergoeconomic analysis plays a key role in determining the optimal performance of a thermodynamic system. By combining exergy analysis and economic principles in a cost-effective method, exergoeconomic analysis can be used to identify the optimum system design via exergy-aided cost minimization. Moreover, due to the consumption of fossil fuels to generate electricity, an environmental analysis that determines the amount of greenhouse gas (GHG) emission is important for analyzing and optimizing such thermodynamic systems. In the present study, exergoeconomic and environmental analyses are applied to the different multistage $CO_2/NH_3$ cascade refrigeration systems. Ammonia is the preferred refrigerant. However, since ammonia is toxic, it is common practice to use carbon dioxide to distribute refrigeration at low temperatures while the high temperatures are served by ammonia in a restricted area. In this study two multistage $CO_2/NH_3$ cascade refrigeration systems equipped with 1) two flash tanks, 2) a flash tank along with flash intercooler with indirect subcooler are proposed. Typically, exergoeconomic and environmental analyses of such systems have not been reported, but are needed to provide a more comprehensive view. Furthermore, the effects on performance and total annual cost for each system are investigated for operational parameters such as evaporator, condenser and cascade heat exchanger outlet temperatures, pressures of the flash tank (FT) or flash intercooler with indirect subcooler (FIS) of the low-temperature circuit, mass flow rate ratio of the FIS and degree of superheating of $CO_2$ at the evaporator outlet. Also an optimization is performed based on maximum COP and exergy efficiency and the minimum total cost rate (including capital, operating and maintenance costs as well as the penalty cost of GHG emission). The objective is to improve understanding of $CO_2/NH_3$ cascade refrigeration systems equipped with flash tanks with or without an indirect subcooler and the benefits that their use can provide.

## 2. System description

Fig. 1(a) provides a schematic of the $CO_2/NH_3$ cascade refrigeration cycle equipped with two flash tanks (system 1). The system consists of the two loops: a high-temperature cycle with $NH_3$ as the working fluid and a low-temperature cycle with $CO_2$ as the working fluid. Both loops are equipped with flash tanks while the one in the $CO_2$ loop has also an intercooler function. A flash intercooler cools the discharge vapor exiting the low-temperature compressor (LTC I) before it enters the LTC II. The vapor cooling is performed within the flash tank by vaporizing some liquid at the pressure maintained in the tank. In the high-temperature cycle, the saturated liquid $NH_3$ from the flash tank flows to the cascade condenser. At the same time, the superheated $CO_2$ vapor from the LTC II enters the cascade condenser. In the cascade heat exchanger, $NH_3$ evaporates to a saturated vapor while $CO_2$ condenses to a saturated liquid. Then, the $NH_3$ vapor from the cascade condenser enters the flash tank, from which saturated $NH_3$ vapor flows to the high-temperature compressor (HTC). In the low-temperature cycle, the saturated $CO_2$ liquid from the cascade condenser, after isenthalpic expansion in throttling valve (TV II), returns to the $CO_2$ flash tank and partially vaporizes due to flashing and cooling of the superheated $CO_2$ vapor from LTC I. The residual $CO_2$ saturated liquid then flows to TV I. The condenser in the high-temperature cycle rejects the heat to the environment at inlet temperature $T_{\mathrm{env,i}}$ and the evaporator in the low-temperature cycle absorbs heat from the cold air at inlet temperature $T_{\mathrm{ca,i}}$. Fig. 1(b) shows the processes occurring in both the high- and low-temperature cycles on a *T*–*s* diagram.

Fig. 2(a) shows a schematic of the $CO_2$/$NH_3$ cascade refrigeration cycle equipped with a flash tank and a flash intercooler with an indirect subcooler (system 2). The $CO_2$ after the cascade heat exchanger is divided into two streams. One is throttled down to the intermediate pressure through TV II and flows into the FIS. Then the $CO_2$ flashes to a vapor, cools the residual stream of high pressure liquid, mixes and exchanges heat with the discharged high temperature $CO_2$ from LTC I. Then the resulting saturated vapor is drawn in to LTC II. The cooled high pressure liquid is expanded in the TV I and then fed to the evaporator. Fig. 2(b) shows the processes on a *T–s* diagram.

## 3. Thermodynamic, economic and environmental analyses

For the thermodynamics and economics analyses of the proposed $CO_2$/$NH_3$ cascade refrigeration system it is assumed that pressure and heat losses in all system components and connections are negligible and that all components operate under steady-state conditions. It is also assumed that nuclear, electric, electromagnetic and surface tension effects are absent and that changes in kinetic and potential energy are negligible. Moreover, there is no subcooling at the outlet of the condenser and cascade heat exchanger.

### *3.1. Energy analysis*

Applying the first law of thermodynamics, a steady-state form of the energy rate balance for the *k*th component of system can be expressed as follows:

$$\dot{Q}_{\mathrm{k}} + \sum_{\mathrm{i}} \left(\dot{m}h\right)_{\mathrm{k}} = \sum_{\mathrm{e}} \left(\dot{m}h\right)_{\mathrm{k}} + \dot{W}_{\mathrm{k}} \tag{1}$$

The cooling load of the system is equal to the heat transfer rate absorbed by the $CO_2$ evaporator and is defined as:

$$\dot{Q}_{\mathrm{EV}} = \dot{m}_1 \left(h_1 - h_8\right) \tag{2}$$

The electric power consumption of the compressor is obtained as:

$$\dot{W}_{\mathrm{CM}} = \frac{\dot{m}\left(h_{\mathrm{es}} - h_{\mathrm{i}}\right)}{\eta_{\mathrm{s}}\eta_{\mathrm{el}}\eta_{\mathrm{m}}} = \frac{\dot{m}\left(h_{\mathrm{es}} - h_{\mathrm{i}}\right)}{\eta_{\mathrm{total}}} \tag{3}$$

where $\eta_{\mathrm{s}}$, $\eta_{\mathrm{el}}$ and $\eta_{\mathrm{m}}$ respectively are the isentropic, electrical and mechanical efficiencies of the compressor. The total isentropic efficiency of the considered compressors, $\eta_{\mathrm{total}}$, is defined as:

For the HTC (ammonia screw compressor) (J.S. Bahamonde, personal communication, February 5, 2012):

$$\eta_{\mathrm{total}} = \begin{cases} 0.0071PR^5 - 0.1264PR^4 + 0.9023PR^3 - 3.2277\,PR^2 + 5.7871PR - 3.3429 & \text{for } PR < 4.3 \\ -0.0261PR + 0.9069 & \text{for } PR \geq 4.3 \end{cases} \tag{4}$$

For the LTC (carbon dioxide piston compressor) (L. Shi, personal communication, October 19, 2015):

$$\eta_{\mathrm{total}} = \begin{cases} -0.1234PR^4 + 1.1251PR^3 - 3.8902PR^2 + 6.0433PR - 2.8860 & \text{for } PR < 2.7 \\ -0.0237PR^4 + 0.3051PR^3 - 1.4740PR^2 + 3.1348PR - 1.7978 & \text{for } PR \geq 2.7 \end{cases} \tag{5}$$

where $PR$ is the pressure ratio of the compressor. Defining the mass flow rate ratio of the flash intercooler as $r = \dot{m}_7/\dot{m}_6$ in system 2, the energy balance equation for the flash intercooler can be written as follows:

$$h_6 + r\left(h_2 + h_5\right) = r\left(h_3 + h_7\right) + h_3 \tag{6}$$

The power consumptions of the evaporator and condenser fans are approximated as follows [19]:

$$\dot{W}_{\mathrm{Fan\ I}} = 0.075\left(\dot{Q}_{\mathrm{EV}}\right) \tag{7}$$

$$\dot{W}_{\mathrm{Fan\ II}} = 0.027\left(\dot{Q}_{\mathrm{EV}} + \sum_j \dot{W}_{\mathrm{CM},\,j}\right) \tag{8}$$

where $\sum_j \dot{W}_{\mathrm{CM},\,j}$ denotes the sum of the electrical power consumptions of the compressors.

The total electrical power consumption of the system can be written as:

$$\dot{W}_{\text{total}} = \dot{W}_{\text{LPC I}} + \dot{W}_{\text{LPC II}} + \dot{W}_{\text{HPC}} + \dot{W}_{\text{Fan I}} + \dot{W}_{\text{Fan II}} \tag{9}$$

167 The COP of the system is defined as:

$$\text{COP} = \frac{\dot{Q}_{\text{EV}}}{\dot{W}_{\text{total}}} \tag{10}$$

168 The total heat transfer area of the heat exchangers is calculated as follows:

$$A = \frac{\dot{Q}}{U_{\text{o}} F \Delta T_{\text{lm}}} \tag{11}$$

169 where $U_{\text{o}}$ and $\Delta T_{\text{lm}}$ are the overall heat transfer coefficient based on external heat transfer
170 area and the logarithmic mean temperature difference (LMTD) of the heat exchanger,
171 respectively. A mathematical relationship to determine the LMTD correction factor, $F$, is
172 given by Fettaka et al. [20]. For counter-flow heat exchangers and the evaporator, the
173 correction factor $F$ has a value of 1 but for the condenser the value of F should be calculated.

174 *3.2. Exergy analysis*

175 When the kinetic and potential energies are neglected, the physical exergy at point *j* in a
176 system can be expressed by:

$$\dot{E}x_j = \dot{m}_j \left[ \left( h - h_0 \right)_j - T_0 \left( s - s_0 \right)_j \right] \tag{12}$$

177 where $T_0$ is the thermodynamic averaged temperature of the ambient environment defined as
178 follows [21]:

$$T_0 = \frac{\left( T_{\text{e}} - T_{\text{i}} \right)_{\text{env}}}{\ln \left( T_{\text{e}} / T_{\text{i}} \right)_{\text{env}}} \tag{13}$$

179 Applying an exergy balance to the *k*th system component, the exergy destruction rate can be
180 defined as follows:

$$\dot{E}x_{\text{D,k}} = \dot{E}x_{\text{F,k}} - \dot{E}x_{\text{P,k}} \tag{14}$$

where the subscripts 'F' and 'P' indicate fuel (or driving input) and product (or desired output), respectively. The exergy efficiency can be expressed as the ratio of product exergy rate to fuel exergy rate:

$$\psi_{\mathrm{k}} = \frac{\dot{E}x_{\mathrm{P,k}}}{\dot{E}x_{\mathrm{F,k}}} \tag{15}$$

Estimations of fuel and product exergy rates for each component of these proposed systems are given in Table 1. For the exergy analysis of the throttling valve, it is necessary to split the physical exergy of the fluid flow into its mechanical and thermal parts [22].

The product exergy rate of the system is the exergy rate of heat transferred to the evaporator:

$$\dot{E}x_{\mathrm{P}} = \dot{E}x_{\mathrm{ca,e}} - \dot{E}x_{\mathrm{ca,i}} \tag{16}$$

the fuel exergy rate of the system is the total electrical power input:

$$\dot{E}x_{\mathrm{F}} = \dot{W}_{\mathrm{total}} \tag{17}$$

Accordingly, the exergy efficiency of the system can be expressed as:

$$\psi = \frac{\dot{E}x_{\mathrm{ca,e}} - \dot{E}x_{\mathrm{ca,i}}}{\dot{W}_{\mathrm{total}}} = 1 - \frac{\dot{E}x_{\mathrm{D,total}}}{\dot{W}_{\mathrm{total}}} \tag{18}$$

*3.3. Economic analysis*

In the economic analysis, a cost rate balance can be expressed for the overall system as follows:

$$\dot{C}_{\mathrm{total}} = \dot{C}_{\mathrm{env}} + \dot{Z}_{\mathrm{OP}} + \sum_{\mathrm{k}} \dot{Z}_{\mathrm{k}} \tag{19}$$

where $\dot{C}_{\mathrm{env}}$ is the rate of penalty cost of GHG emission for the *k*th component (see section 3.4). The operating cost of the system, $\dot{Z}_{\mathrm{OP}}$, including the cost of electricity consumption, can be defined as follows:

$$\dot{Z}_{\mathrm{OP}} = N \times \dot{W}_{\mathrm{total}} \times \alpha_{\mathrm{el}} \tag{20}$$

where $N$ is the yearly number of operation hours of the system and $\alpha_{\text{el}}$ is the unit electricity cost in \$ kWh$^{-1}$. The rate of capital investment and maintenance costs of each system component can be estimated as follows [23]:

$$\dot{Z}_k = \frac{Z_k \times \phi}{N \times 3600}\text{CRF} \tag{21}$$

where $Z_{\text{k}}$ is the capital cost of the $k$th component and $\phi$ is the maintenance factor. The capital recovery factor (CRF) is defined as [24]:

$$\text{CRF} = \frac{i(1+i)^n}{(1+i)^n - 1} \tag{22}$$

where $i$ and $n$ are the annual interest rate and system life time, respectively.

Exergy destructions and capital costs are the real cost sources of a thermodynamic system. In an exergoeconomic evaluation, the exergoeconomic factor expresses the relative significance of a component and can be defined as follows [25]:

$$f_{\text{k}} = \frac{\dot{Z}_{\text{k}}}{\dot{Z}_{\text{k}} + c_{\text{F,k}}\,\dot{E}x_{\text{D,k}}} \tag{23}$$

where $c_{\text{F,k}}$ is the unit cost of fuel for the $k$th component and can be calculated by solving the exergy cost rate balance for the $k$th component, which can be expressed in a general form as [24]:

$$\sum_{\text{e}}\left(c\dot{E}x\right)_{\text{k}} = \sum_{\text{i}}\left(c\dot{E}x\right)_{\text{k}} + \dot{C}_{\text{env,k}} + \dot{Z}_{\text{k}} + \dot{Z}_{\text{OP,k}} \tag{24}$$

where $c$ is the unit cost of exergy in each flow. In this study, external exergy losses are not considered and the thermodynamic inefficiencies of a component consist exclusively of exergy destruction [26]. A low value of $f_{\text{k}}$ calculated for a major component suggests that cost savings in the entire system might be achieved by improving the component efficiency even if it increases the capital investment for the component. Conversely, a high value of $f_{\text{k}}$

suggests a decrease in the investment costs of this component at the expense of its exergetic efficiency may be reasonable [24].

*3.4. Environmental analysis*

The rate of penalty cost of GHG emission for the considered system can be determined based on the annual amount of GHG emission from the system, $m_{CO_2e}$, as follows [27]

$$\dot{C}_{env} = m_{CO_2e} c_{CO_2} \tag{25}$$

where $c_{CO_2}$ is the cost of $CO_2$ avoided and $m_{CO_2e}$ is obtained as:

$$m_{CO_2e} = \mu_{CO_2e} \times E_{annual} \tag{26}$$

Here, $\mu_{CO_2e}$ is the emission factor and $E_{annual}$ is the annual electrical energy consumption of the system in kWh.

## 4. System specifications

To determine the investment cost rate of each component, the maintenance factor ($\phi$) is 1.06 and the investment cost ($Z_k$) can be estimated based on the cost functions listed in Table 2. In calculating the CRF, the annual interest rate ($i$), the life time of the system ($n$) are considered as 14% and 15 years respectively. The average electricity cost is 0.09 \$ kWh$^{-1}$ (Iran's electricity tariff in 2015) and the annual operational hours of the system ($N$) are considered to be 4266 h [19]. The emission factor of electricity ($\mu_{CO_2e}$) is taken to be 0.968 kg kWh$^{-1}$ (Iran's average) and the cost of $CO_2$ avoided ($c_{CO_2}$) is considered as 87 \$ ton$^{-1}$ of $CO_2$e emissions for the natural gas combined cycle power plants with post-combustion capture technology [28]. Thermodynamic conditions of the system are listed in Table 3.

## 5. Results and discussion

The validation for a basic $CO_2/NH_3$ cascade refrigeration system is shown in Table 4. Good agreement is observed between the obtained results for performance parameters of the system and the corresponding results reported in References [18] and [29]. However, since Ref. [18] does not consider the cost of condenser and evaporator fans, the predicted value of the total cost rate for the present model is 1.3% higher than reported in Ref. [18].

Fig. 3 shows the variations of system COP and exergy efficiency with evaporating temperature of the $CO_2$ for the two proposed $CO_2/NH_3$ cascade refrigeration systems. In obtaining these results, other operating parameters are kept constant. Since the thermodynamic averaged temperature of the ambient environment and the cooled space are fixed, the trend of COP variation is the same as for that of the exergy efficiency. Due to the minimum allowable temperature difference of 5 K in the flash intercooler with an indirect subcooler, the mass flow rate ratio, $r$, should be greater than 3.2. As expected, an increase in evaporating temperature decreases the pressure ratio of LTC I and the total electrical power consumption. Therefore, the system COP and exergy efficiency both increase. Moreover, in system 2, an increase of $r$ leads to a rise in mass flow rate through LTC I, which increases the compression work and causes the COP and exergy efficiency to decrease. Under the given conditions for system 1, a 10 K increase in $T_{EV}$ from −45 °C to −35 °C leads to increases of 16.9% in both COP and exergy efficiency. At the same condition for system 2, a 10 K increase in $T_{EV}$ leads to a maximum increase of 20.8% in both COP and exergy efficiency when $r = 3.6$. Also, it can be seen from Fig. 3 that, due to the lower electrical power consumption, the COP and exergy efficiency of system 1 are greater than for system 2, under the same operating conditions.

The effect of varying the evaporating temperature of the $CO_2$ on the ratio of the penalty cost of GHG emission and the total annual cost rate is shown in Fig. 4. By increasing the $CO_2$ evaporating temperature, the electrical power consumption of LTC I decreases and leads to a reduction in the $\dot{C}_{env}$. Also, by increasing the $CO_2$ evaporating temperature, the heat transfer surface area of the evaporator increases and leads to an increase in the system capital and total costs above a certain value of $T_{EV}$. It is also observed that, under the same operating conditions, the total cost rate of system 2 exceeds that of system 1, as a result of the higher capital cost of FIS. For instance, using FT in the $CO_2$ circuit leads to a decrease of up to 14.3% in the total cost rate in comparison with system 2 at $T_{EV} = -45$ °C.

Fig. 5 shows the variation of the COP and exergy efficiency of the system with condensing temperature of the $NH_3$ for the proposed $CO_2/NH_3$ refrigeration systems. These results are obtained with the other operating parameters kept constant. An increase in condensing temperature is seen to increase the pressure ratio of the HTC and the total electrical power consumption and leads to decreases in the system COP and exergy efficiency. For system 1, a 10 K increase in $T_{CD}$ leads to a 13.4% decrease in both COP and exergy efficiency. At the same condition for system 2, a 10 K increase in $T_{CD}$ leads to maximum decrease of 13.3% in both COP and exergy efficiency when $r = 3.2$. Moreover, using a FIS with $r = 3.2$ in the system leads to decreases of up to 1.2% for both system COP and exergy efficiency relative to system 1, at a condensing temperature 35 °C.

Fig. 6 shows the effect of varying the condensing temperature of $NH_3$ on the ratio cost rate due to GHG emission and the total annual cost rate. By increasing the $NH_3$ condensing temperature, the electrical power consumption of the HTC increases and leads to an increment in $\dot{C}_{env}$. It can be seen that variations of the ratio of penalty cost of GHG emission to $r$ is negligible for system 2, due to the small effect of $r$ on the performance of the $NH_3$ circuit. Also, by increasing the $NH_3$ condensing temperature, the total costs of the HTC increase due to the increased electrical power consumption, leading to an increase of the total cost rate of the system. In systems 1 and 2, a 10 K increase in $T_{CD}$ leads to 4.8% and 4.2%

increases respectively in total cost rate. Furthermore, using an open intercooler in the $CO_2$ circuit leads to decreases of almost 13% for the total annual cost rate in comparison to system 2.

Fig. 7 illustrates the variation of system COP and exergy efficiency with the cascade temperature difference of the systems, $\Delta T_{CAS}(=T_5 - T_{13})$. An increase in cascade temperature difference raises the pressure ratio of the HTC and the total electrical power consumption, while the condensing temperatures of $CO_2$ in the cascade heat exchanger and $NH_3$ in condenser are kept constant. Therefore, system COP and exergy efficiency both decrease. Under the given conditions, a 10 K increase in $\Delta T_{CAS}$ from 2 K to 12 K leads to decreases of 14.6% and up to 14.5% for systems 1 and 2, respectively, in both COP and exergy efficiency. It can also be seen in Fig. 7 that using a flash intercooler with $r = 3.2$ in the system leads to 1.3% decreases in both COP and exergy efficiency when the cascade temperature difference is set to 2 K.

The effect of varying the cascade heat exchanger temperature difference on the ratio of GHG emission cost rate and total annual cost rate is shown in Fig. 8. Increasing the cascade heat exchanger temperature difference is seen to raise the ratio GHG emission cost rate and total cost rate, due to an increase of the capital and operating costs of the HTC which in turn is a result of the electrical power consumption increase. For system 1, a 10 K increase in $\Delta T_{CAS}$ leads up to 5.7% increase in $\dot{C}_{total}$. For the system 2, a 10 K increase in $\Delta T_{CAS}$ leads to an increase of 5.4% in $\dot{C}_{total}$ when $r$ =3.2. Also using a FT in the system leads to a decrease of up to 13.2% in $\dot{C}_{total}$ in comparison with system 2 at $\Delta T_{CAS} = 2$ K.

Fig. 9 illustrates the variation of the COP and exergy efficiency of the system with condensing temperature of the $CO_2$ in the cascade heat exchanger, $T_5$, for the presented systems. These results are obtained while other operating parameters are kept constant. Since the minimum temperature difference in the flash intercooler with an indirect subcooler should be greater than 5 K, the lower limit of $T_5$ is considered as 0 °C. An increase in $T_5$ leads to an increase in pressure ratio of the LTC II and a decrease in pressure ratio of the HTC since $\Delta T_{CAS}$, $T_{CD}$ and $P_{int}$ are held constant. As long as the reduction in HTC power is greater than the increase in LTC II power ($T_5$ is less than 2 °C), COP and exergy efficiency increase. When the increment in LTC II power is greater than the reduction in HTC power, COP and exergy efficiency decrease.

The effect of varying the condensing temperature of the $CO_2$ in the cascade heat exchanger on the ratio of cost rate due to GHG emission and total annual cost rate is shown in Fig. 10. The results show that, when $T_5$ is less than 2 °C, due to the reduction in total electrical power consumption, the capital and operating costs of the system decline in both systems, while other operating parameters are kept constant. After that, due to the increment in total electrical power consumption, $\dot{C}_{env}$ and $\dot{C}_{total}$ increase. Fig. 10 (a) shows that the ratio of cost rate due to GHG emission decreases with increasing condensing temperature of the $CO_2$ due to the decreased power consumption and GHG emission. Although the COP and exergy efficiency are less sensitive to the use of an FT instead of an FIS in the $CO_2$ circuit, the total cost rate depends on this choice. System 1 leads to a 18.4% decrease in the total cost rate at $T_5$=10 °C in comparison to system 2.

Fig. 11 shows the variation of the COP and exergy efficiency of the system with the intermediate pressure for the $CO_2$ low-temperature circuit. Due to the increase and decrease in the electrical power consumption of LTC I and LTC II respectively, which result from the variation of pressure ratio, an optimal $P_{int}$ is seen to exist which leads to a maximum COP and exergy efficiency. The optimum value of $P_{int}$ is sensitive to the evaporating and condensing temperatures of $CO_2$ in the low-temperature circuit. However, using system 1 instead of system 2 leads to an increase in the optimum value of $P_{int}$ while $T_{EV}$ and $T_5$ are kept constant. The results also show that the mass flow rate ratio $r$ has a negligible effect on COP and exergy efficiency for system 2.

The effect of the intermediate pressure for the $CO_2$ low-temperature circuit on the ratio of the cost rate due to GHG emission and the total annual cost rate is shown in Fig. 12, where it is observed that, at the optimal $P_{int}$, the lowest penalty cost of GHG emission and total cost rate are obtained. In this case, the total cost rate for system 1 is 13.3% less than that for system 2. Also, it can be seen that the ratio of cost rate due to GHG emission for system 2 is 2.9% less than that for system 1 when both systems operate at the optimal $P_{int}$. This indicates that the investment, operating and maintenance costs of system 2 exceed those for system 1.

Fig. 13 shows the variation of system COP and exergy efficiency with superheating degree of $CO_2$ at evaporator outlet. A small decrease of mass flow rate and a large increase in specific consumed work of LPC I lead to decreases in the COP and exergy efficiency. Under the given conditions, a 10 K increase in $\Delta T_{sup}$ from 0 to 10 K leads to decreases of 0.9% and up to 2.3% for systems 1 and 2, respectively, in both COP and exergy efficiency. Furthermore, system 1 leads to increases of up to 3.8% for both system COP and exergy efficiency in comparison to system 2, at $\Delta T_{sup} = 10$ K.

Fig. 14 illustrates the effect of varying degree of superheating of $CO_2$ at the evaporator outlet on the ratio of cost rate due to GHG emission and total annual cost rate. By increasing the $CO_2$ superheating degree, the electrical power consumption of LTC I and the heat transfer surface area of the evaporator increase, leading to a rise in both the penalty cost rate of GHG emission and the system capital and total costs.

Fig. 15 displays the variation of the ratio of GHG emission cost rate and total annual cost rate with the cost of $CO_2$ avoided. The cost of $CO_2$ avoided varies significantly for different types of power plants [28]. The results show that the penalty cost rate of GHG emission and total cost rate are sensitive to $c_{CO_2}$. For system 1, increasing the cost of $CO_2$ avoided from 30 \$ ton$^{-1}$ of $CO_2$e to 120 \$ ton$^{-1}$ of $CO_2$e (300%) leads to an increase of 29.7% and 25.5% in total cost rate for systems 1 and 2, respectively.

In order to optimize the performances of systems 1 and 2, from the thermodynamic and economic viewpoints, the DIRECT algorithm in the EES software has been used. The values of operating parameters for the thermodynamic optimal design case and parameters affecting the total annual cost are for the cost optimal design case are summarized in Tables 5 and 6, respectively. The results of thermodynamic and economic optimizations show that the values of COP and exergy efficiency for the compared systems are almost the same. Yet, the total annual cost rate for system 1 is 11.2% and 11.9% lower than that for system 2 referring to thermodynamic and economic optimizations, respectively. Comparing the thermodynamic and cost optimal design conditions for system 1, an increase of 14.8% in COP and exergy efficiency is achieved at the expense of a 3.0% increment in the total annual cost rate, when the optimization is based on the maximum COP. This comparison for system 2 shows an increase of 11.6% in COP and exergy efficiency and 2.1% in the total annual cost rate.

Fig. 16 shows the values of exergy destruction ratio for various components of the proposed cascade cycles at thermodynamically optimal design condition. As can be seen, the highest value of exergy destruction rate is attributable to Fan I in both cycles (44.9 kW). The high mass flow rate and a temperature of cooled air lower than the ambient temperature lead to a high entropy generation and so a high irreversibility for Fan I. After that, LTC II of both cycles has the highest value of exergy destruction rate (31.1 kW in system 1 and 26.8 kW in system 2), due to the compression process. After $NH_3$ flash tank, the lowest value of exergy destruction rate is associated with the $CO_2$ flash tank for system 1 (2.7 kW) and TV II for the system 2 (1.6 kW) due to negligible heat losses and a throttling process at low pressure.

Fig. 17 displays the values of exergy destruction ratio for various components of cascade systems 1 and 2 at cost optimal design condition. After Fan I with its exergy destruction rate of 44.9 kW, the evaporator of both cycles has the highest value of exergy destruction rate (41.1 kW), due to the large temperature difference between the cooled air and $CO_2$. The results obtained from the exergoeconomic analysis of the $CO_2/NH_3$ cascade refrigeration, systems 1 and 2, for the thermodynamic and economic optimum conditions are presented in Tables 7 and 8, respectively. The results of both thermodynamic and economic optimizations show that, after the $NH_3$ flash tank in the compared cycles, the $CO_2$ flash tank has the highest value of exergy efficiency for system 1 (about 97%) and the FIS the highest value for system 2 (about 92%). The lowest exergy efficiencies are observed for the Fan II (1.67%) and condenser (about 3%) for both cycles. For thermodynamic and economic optimum conditions, the low value of $f$ for the flash tank of system 1 (about 1.8%) and cascade heat exchanger in the system 2 (about 3%) indicate that the costs associated with these components are almost exclusively due to exergy destructions. The exergoeconomic factor of the $NH_3$ flash tank of 100% for both cycles and the relatively large value of $f$ for the evaporator in system 1 suggests that the capital investment, operating and maintenance costs dominate.

## 6. Conclusions

Exergoeconomic and environmental analyses are successfully carried out for two different $CO_2/NH_3$ cascade refrigeration systems equipped with two flash tanks and a flash tank along with a flash intercooler with an indirect subcooler. To determine the maximum value of COP and exergy efficiency and the minimum cost rate due to GHG emission and total cost rate of the system, the following operating parameters are considered: condensing temperature of $NH_3$ in condenser and $CO_2$ in cascade heat exchanger, evaporating temperature of $CO_2$ in evaporator, temperature difference in the cascade heat exchanger, intermediate pressure in the

$CO_2$ low-temperature circuit and mass flow rate ratio of the FIS. From the energy, exergy, economic and environmental analyses the following results are obtained and conclusions drawn:

- By using the FIS in $CO_2$ low-temperature circuit instead of the FT, the performance of the $CO_2/NH_3$ cascade refrigeration system is decreased.
- For system 1, a 10 K increase in $T_{EV}$ leads to increases of 16.9% in both COP and exergy efficiency. At the same conditions for system 2, a 10 K increase in $T_{EV}$ leads to maximum increase of 20.8% in both COP and exergy efficiency when $r = 3.6$. Also, using a FIS in the system leads to an increase of 14.3% in the total cost rate.
- The minimum annual total cost rate is obtained at a $CO_2$ evaporating temperature of −41.5 °C and −40 °C, respectively for systems 1 and 2 when $r = 3.2$.
- For system 1, a 10 K increase in $T_{CD}$ leads to a 13.4% decrease in both COP and exergy efficiency. At the same condition for system 2, a 10 K increase in $T_{CD}$ leads to maximum decrease of 13.3% in both COP and exergy efficiency when $r = 3.2$. Also, in systems 1 and 2, a 10 K increase in $T_{CD}$ leads to a 4.8% and 4.2% increase respectively in total cost rate.
- The maximum COP and exergy efficiency are obtained at a $CO_2$ condensing temperature of 1.9 °C and 2.1 °C, respectively for systems 1 and 2 when $r = 3.2$.
- The total annual cost rate for the system 1 is 11.2% and 11.9% lower than that for the system 2 referring to thermodynamic and economic optimizations, respectively.
- The lowest value of the exergoeconomic factor is 1.73% for $CO_2$ flash tank in system 1 and 3.85% for cascade heat exchanger in system 2, demonstrating that the costs associated with $CO_2$ flash tank and cascade heat exchanger in systems 1 and 2 respectively are almost exclusively due to exergy destruction.

- The highest exergoeconomic factor is observed to be 100% for the $NH_3$ flash tank in both systems, suggesting that the capital investment, operating and maintenance costs of the FT in the high-temperature circuit dominate in such cases.

The present study demonstrates the benefits and profitability of $CO_2/NH_3$ cascade refrigeration systems equipped with a flash tank and a flash intercooler, with and without an indirect subcooler. However, a more detailed system design considering heat and pressure losses in all system components and using more accurate cost functions are suggested for further investigation.

## References


[1] I. Dincer, M. Kanoglu, Refrigeration systems and applications, Wiley, 2010.

[2] H.J. Dakkama, A. Elsayed, R.K. Al-Dadah, S.M. Mahmoud, P. Youssef, Investigation of cascading adsorption refrigeration system with integrated evaporator-condenser heat exchanger using different working pairs, Energy Procedia. 75 (2015) 1496–1501. doi:10.1016/j.egypro.2015.07.285.

[3] A.M. Dubey, S. Kumar, G. Das Agrawal, Thermodynamic analysis of a transcritical CO2/propylene (R744–R1270) cascade system for cooling and heating applications, Energy Convers. Manag. 86 (2014) 774–783. doi:10.1016/j.enconman.2014.05.105.

[4] W. Han, L. Sun, D. Zheng, H. Jin, S. Ma, X. Jing, New hybrid absorption–compression refrigeration system based on cascade use of mid-temperature waste heat, Appl. Energy. 106 (2013) 383–390. doi:10.1016/j.apenergy.2013.01.067.

[5] V. Jain, S.S. Kachhwaha, G. Sachdeva, Thermodynamic performance analysis of a vapor compression–absorption cascaded refrigeration system, Energy Convers. Manag. 75 (2013) 685–700. doi:10.1016/j.enconman.2013.08.024.

[6] A. Kilicarslan, M. Hosoz, Energy and irreversibility analysis of a cascade refrigeration system for various refrigerant couples, Energy Convers. Manag. 51 (2010) 2947–2954. doi:10.1016/j.enconman.2010.06.037.

[7] C.A. Infante Ferreira, R.A. Boukens, Carbon dioxide – secondary coolant or refrigerant for cascade systems?, in: Proc. IIR Conf. Appl. Nat. Refrig., Aarhus, Denmark, Denmark, 1996: pp. 185–194.

[8] T.S. Lee, C.H. Liu, T.W. Chen, Thermodynamic analysis of optimal condensing temperature of cascade-condenser in $CO_2/NH_3$ cascade refrigeration systems, Int. J. Refrig. 29 (2006) 1100–1108. doi:10.1016/j.ijrefrig.2006.03.003.

[9] H.M. Getu, P.K. Bansal, Thermodynamic analysis of an R744-R717 cascade refrigeration system, Int. J. Refrig. 31 (2008) 45–54. doi:10.1016/j.ijrefrig.2007.06.014.

[10] J.A. Dopazo, J. Fernández-Seara, J. Sieres, F.J. Uhía, Theoretical analysis of a $CO_2$-$NH_3$ cascade refrigeration system for cooling applications at low temperatures, Appl.

Therm. Eng. 29 (2009) 1577–1583. doi:10.1016/j.applthermaleng.2008.07.006.

[11] W. Bingming, W. Huagen, L. Jianfeng, X. Ziwen, Experimental investigation on the performance of $NH_3/CO_2$ cascade refrigeration system with twin-screw compressor, Int. J. Refrig. 32 (2009) 1358–1365. doi:10.1016/j.ijrefrig.2009.03.008.

[12] J.A. Dopazo, J. Fernández-Seara, Experimental evaluation of a cascade refrigeration system prototype with $CO_2$ and $NH_3$ for freezing process applications, Int. J. Refrig. 34 (2011) 257–267. doi:10.1016/j.ijrefrig.2010.07.010.

[13] M. Ma, J. Yu, X. Wang, Performance evaluation and optimal configuration analysis of a $CO_2/NH_3$ cascade refrigeration system with falling film evaporator–condenser, Energy Convers. Manag. 79 (2014) 224–231. doi:10.1016/j.enconman.2013.12.021.

[14] R.S. Mitishita, E.M. Barreira, C.O.R. Negrão, C.J.L. Hermes, Thermoeconomic design and optimization of frost-free refrigerators, Appl. Therm. Eng. 50 (2013) 1376–1385. doi:10.1016/j.applthermaleng.2012.06.024.

[15] H. Esen, M. Inalli, M. Esen, Technoeconomic appraisal of a ground source heat pump system for a heating season in eastern Turkey, Energy Convers. Manag. 47 (2006) 1281–1297. doi:10.1016/j.enconman.2005.06.024.

[16] H. Esen, M. Inalli, M. Esen, A techno-economic comparison of ground-coupled and air-coupled heat pump system for space cooling, Build. Environ. 42 (2007) 1955–1965. doi:10.1016/j.buildenv.2006.04.007.

[17] H. Esen, M. Inalli, M. Esen, K. Pihtili, Energy and exergy analysis of a ground-coupled heat pump system with two horizontal ground heat exchangers, Build. Environ. 42 (2007) 3606–3615. doi:10.1016/j.buildenv.2006.10.014.

[18] O. Rezayan, A. Behbahaninia, Thermoeconomic optimization and exergy analysis of $CO_2/NH_3$ cascade refrigeration systems, Energy. 36 (2011) 888–895. doi:10.1016/j.energy.2010.12.022.

[19] H. Wijbenga, M. Van Der Hoff, M. Janssen, C.A. Infante Ferreira, Life cycle performance of refrigeration systems in the Dutch food and beverages sector, in: 4th IIR Conf. Thermophys. Prop. Transf. Process. Refrig., Delft, The Netherlands, The Netherlands, 2013.

[20] S. Fettaka, J. Thibault, Y. Gupta, Design of shell-and-tube heat exchangers using multiobjective optimization, Int. J. Heat Mass Transf. 60 (2013) 343–354. doi:10.1016/j.ijheatmasstransfer.2012.12.047.

[21] C.A. Infante Ferreira, Refrigeration and heat pumping in food processing plants, in: L. Stougie (Ed.), Energy Effic. Qual. Energy Food Process. Ind., Interduct: Delft University of Technology, Delft, The Netherlands, 2002: pp. 57–79.

[22] T. Morosuk, G. Tsatsaronis, Advanced exergetic evaluation of refrigeration machines using different working fluids, Energy. 34 (2009) 2248–2258. doi:10.1016/j.energy.2009.01.006.

[23] M. Navidbakhsh, A. Shirazi, S. Sanaye, Four E analysis and multi-objective optimization of an ice storage system incorporating PCM as the partial cold storage for air-conditioning applications, Appl. Therm. Eng. 58 (2013) 30–41. doi:http://dx.doi.org/10.1016/j.applthermaleng.2013.04.002.

[24] A. Bejan, G. Tsatsaronis, M.J. Moran, Thermal design and optimization, Wiley, 1996.

[25] F. Cziesla, G. Tsatsaronis, Z. Gao, Avoidable thermodynamic inefficiencies and costs in an externally fired combined cycle power plant, Energy. 31 (2006) 1472–1489.

doi:10.1016/j.energy.2005.08.001.

[26] G. Tsatsaronis, M.-H. Park, On avoidable and unavoidable exergy destructions and investment costs in thermal systems, Energy Convers. Manag. 43 (2002) 1259–1270. doi:http://dx.doi.org/10.1016/S0196-8904(02)00012-2.

[27] J. Wang, Z. Zhai, Y. Jing, C. Zhang, Particle swarm optimization for redundant building cooling heating and power system, Appl. Energy. 87 (2010) 3668–3679. doi:http://dx.doi.org/10.1016/j.apenergy.2010.06.021.

[28] E.S. Rubin, J.E. Davison, H.J. Herzog, The cost of $CO_2$ capture and storage, Int. J. Greenh. Gas Control. 40 (2015) 378–400. doi:10.1016/j.ijggc.2015.05.018.

[29] M. Aminyavari, B. Naja, A. Shirazi, F. Rinaldi, Exergetic, economic and environmental (3E) analyses, and multi- objective optimization of a $CO_2/NH_3$ cascade refrigeration system, Appl. Therm. Eng. 65 (2014) 42–50. doi:10.1016/j.applthermaleng.2013.12.075.

[30] G. Xu, F. Liang, Y. Yang, Y. Hu, K. Zhang, W. Liu, An improved $CO_2$ separation and purification system based on cryogenic separation and distillation theory, Energies. 7 (2014) 3484–3502. doi:10.3390/en7053484.

[31] S. Sanaye, A. Shirazi, Four E analysis and multi-objective optimization of an ice thermal energy storage for air-conditioning applications, Int. J. Refrig. 36 (2012) 1–14. doi:10.1016/j.ijrefrig.2012.10.014.

[32] A.H. Mosaffa, L. Garousi Farshi, Exergoeconomic and environmental analyses of an air conditioning system using thermal energy storage, Appl. Energy. 162 (2016) 515–526. doi:10.1016/j.apenergy.2015.10.122.

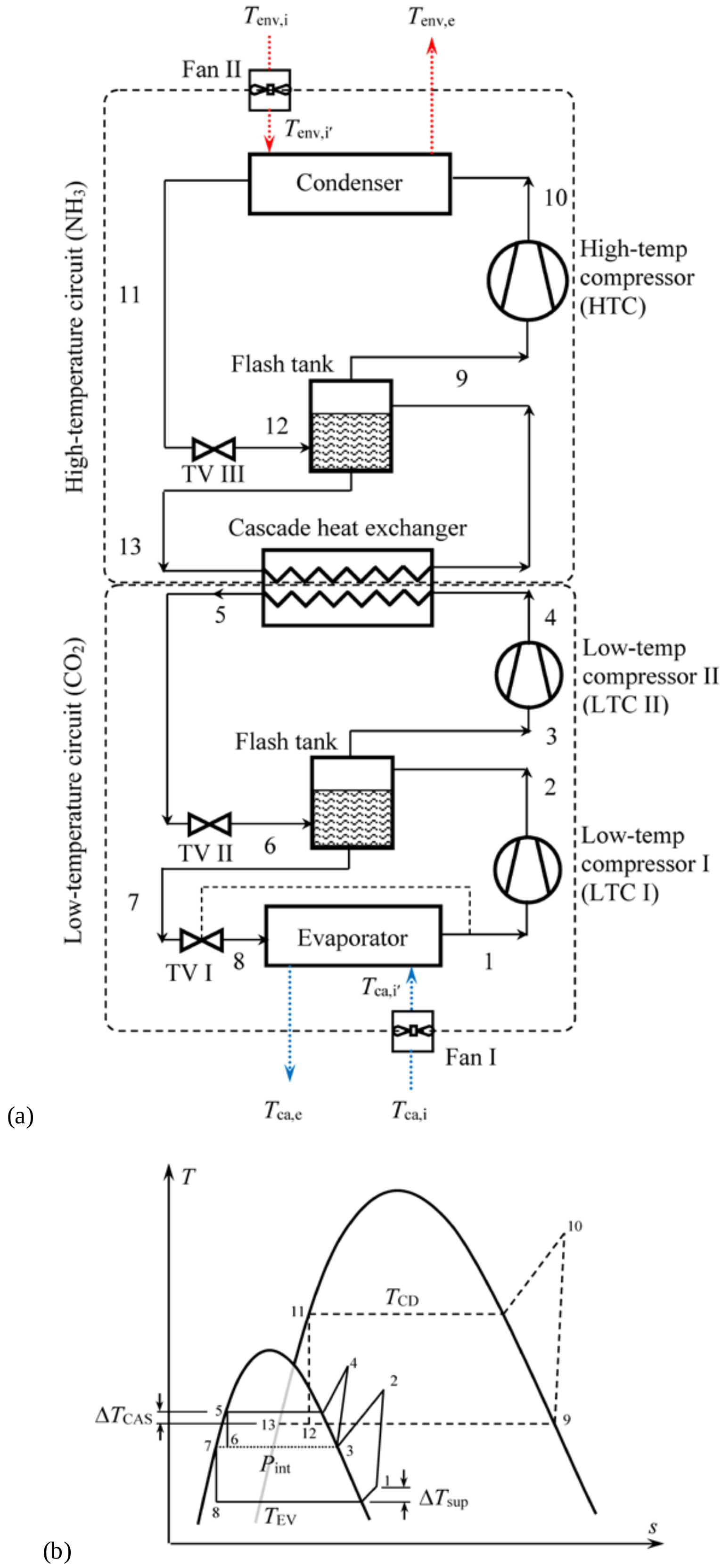


Fig. 1. (a) Schematic and (b) *T-s* diagram for the $CO_2/NH_3$ cascade refrigeration cycle equipped with two flash tanks (system 1).

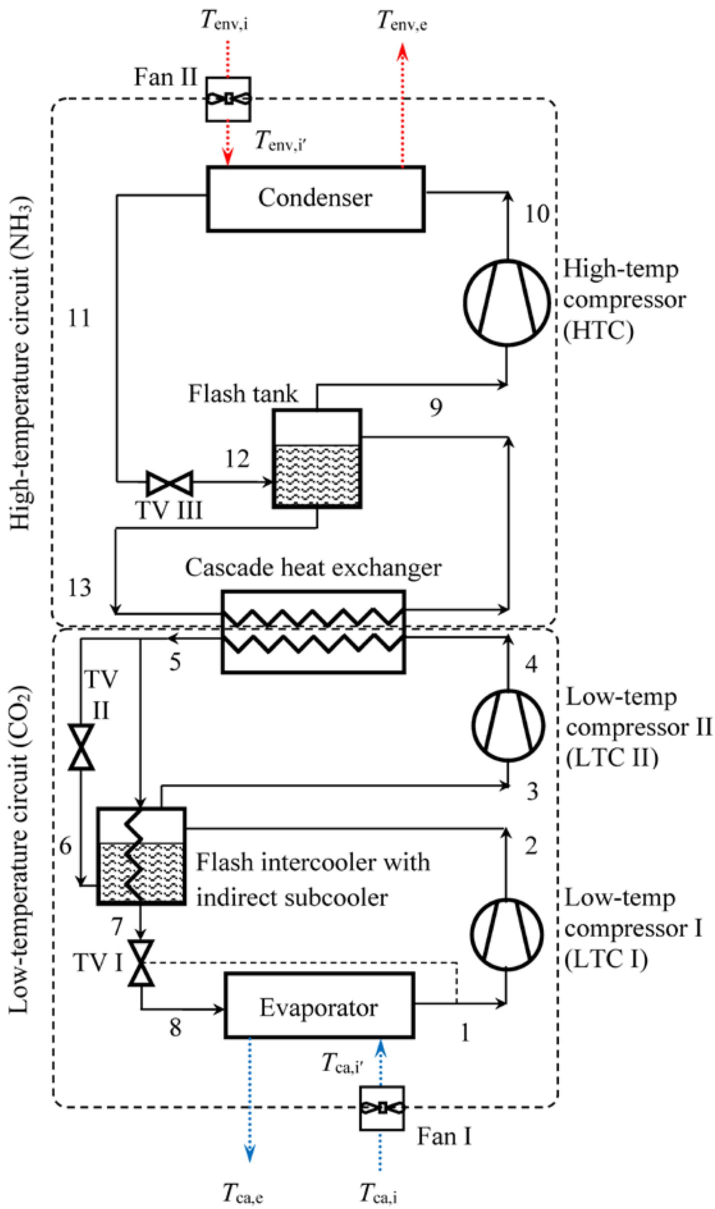


(a)

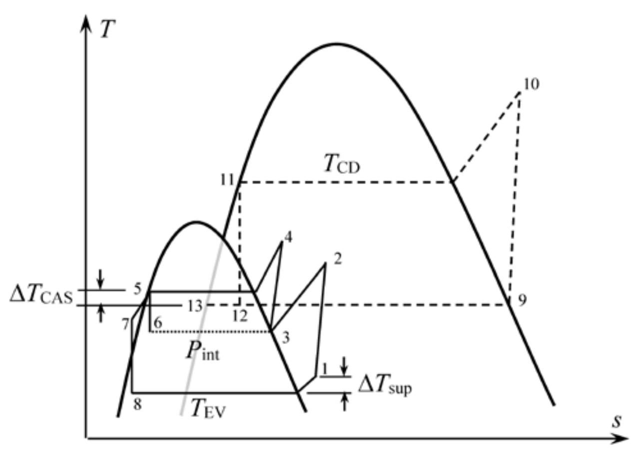


(b)

Fig. 2. (a) Schematic and (b) *T-s* diagram for the $CO_2/NH_3$ cascade refrigeration cycle equipped with a flash tank and a flash intercooler with an indirect subcooler (system 2).

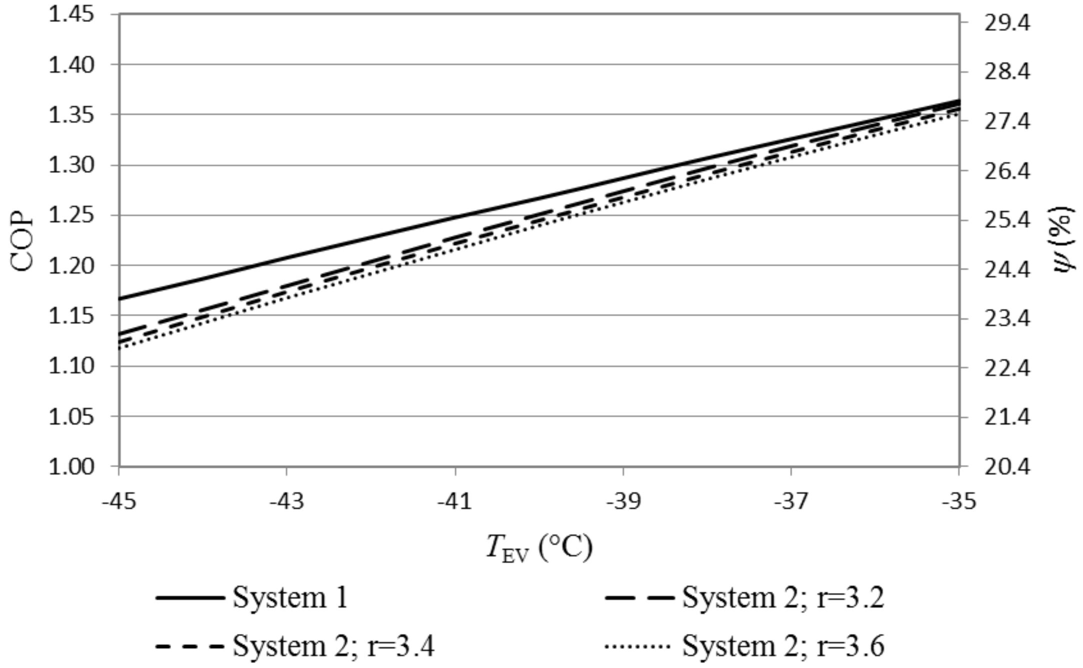


Fig. 3. Variation of system COP and exergy efficiency with $CO_2$ evaporating temperature.

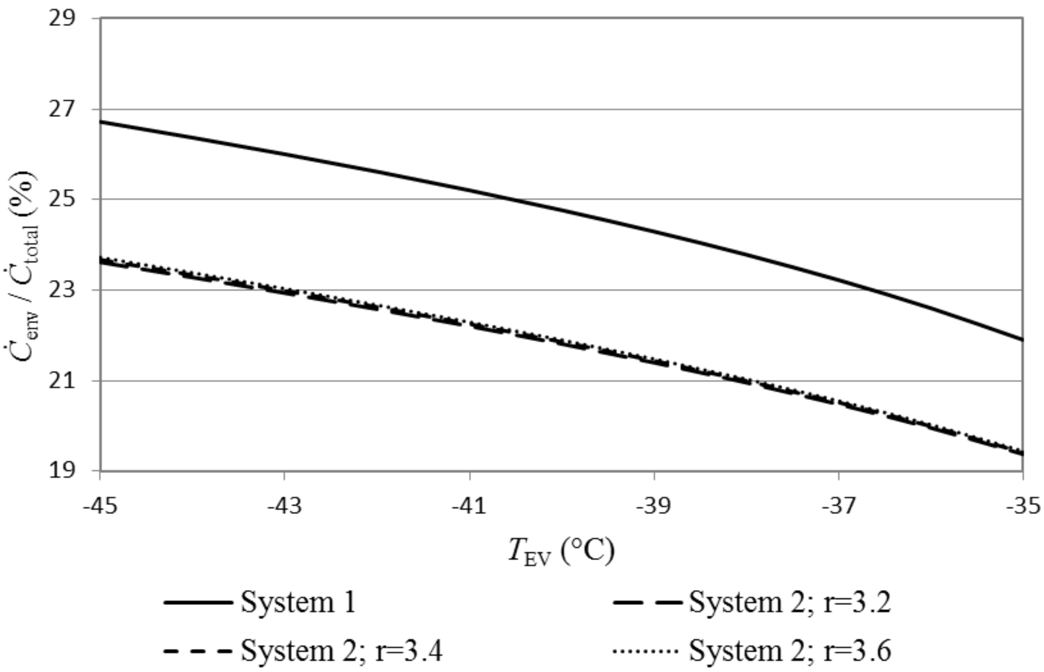


(a)

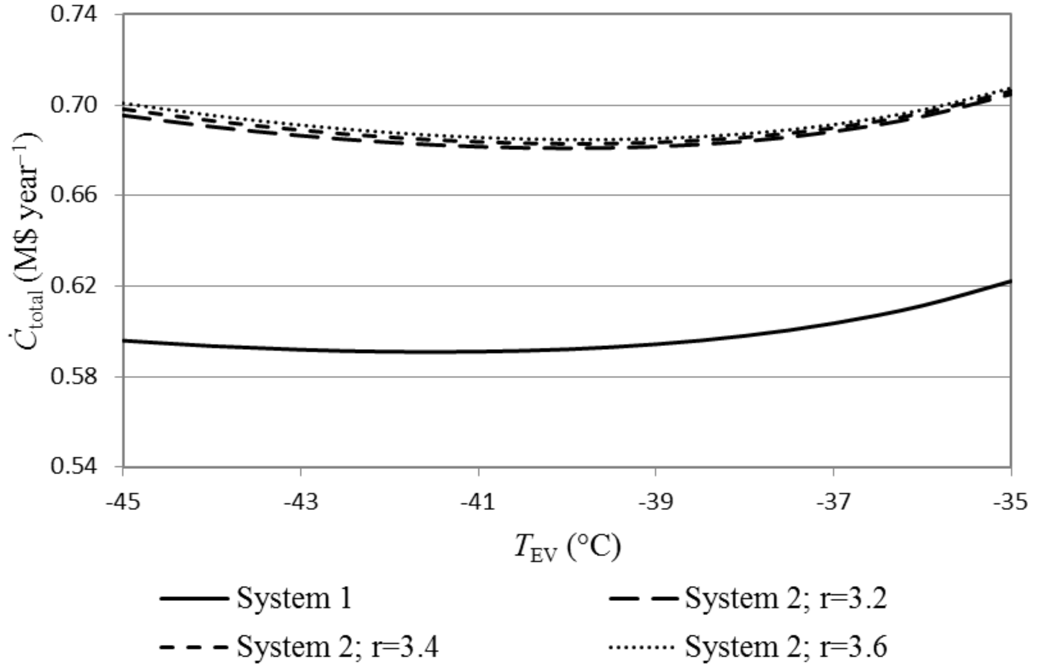


(b)

Fig. 4. Effect of $CO_2$ evaporating temperature on (a) the ratio of penalty cost of GHG emission and (b) the total annual cost rate.

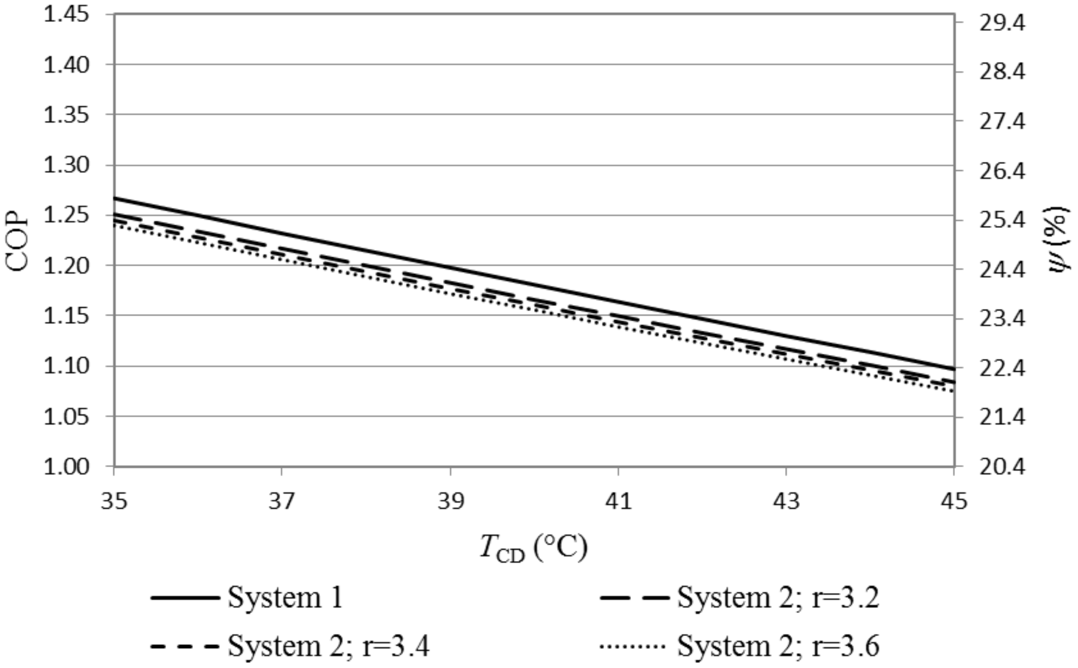


Fig. 5. Variation of system COP and exergy efficiency with $NH_3$ condensing temperature.

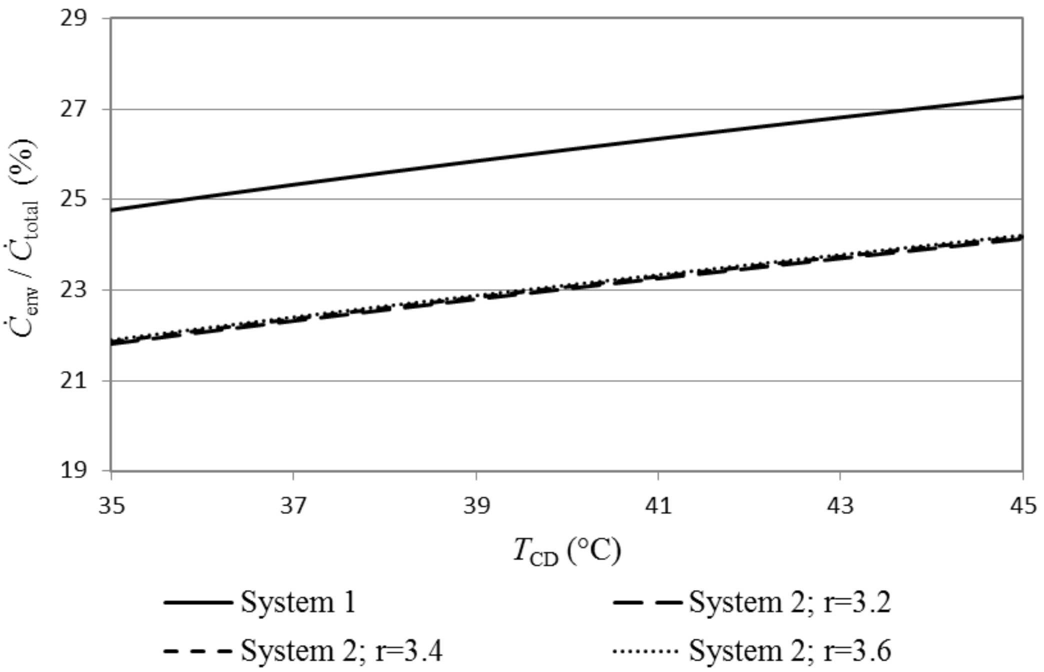


(a)

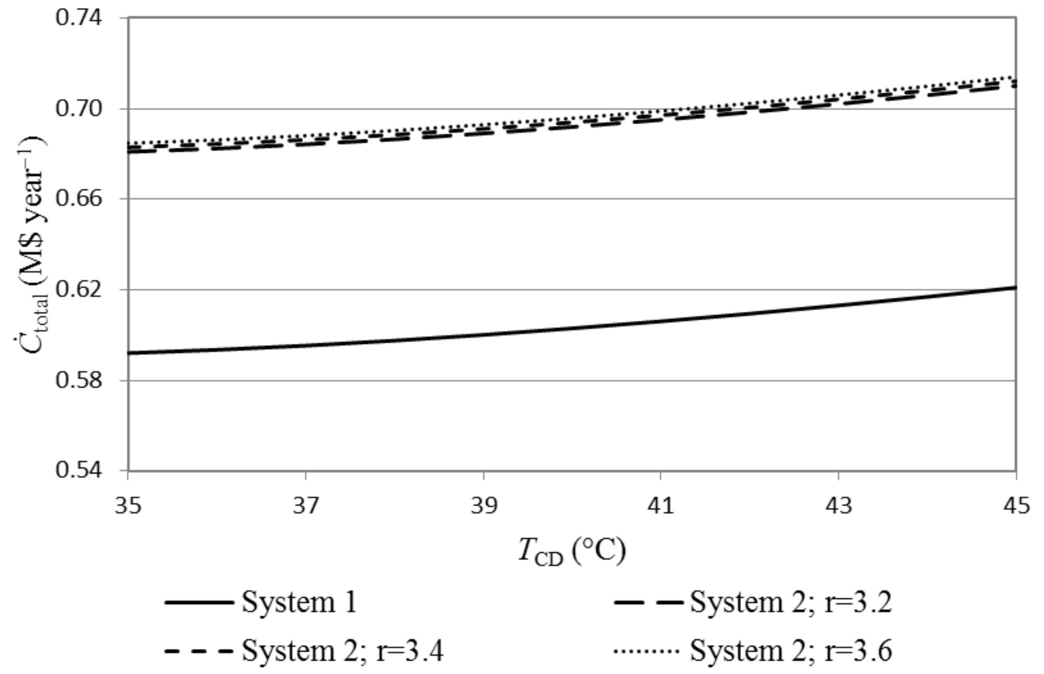


(b)

Fig. 6. Effect of varying $NH_3$ condensing temperature on (a) the ratio of penalty cost of GHG emission and (b) the total annual cost rate.

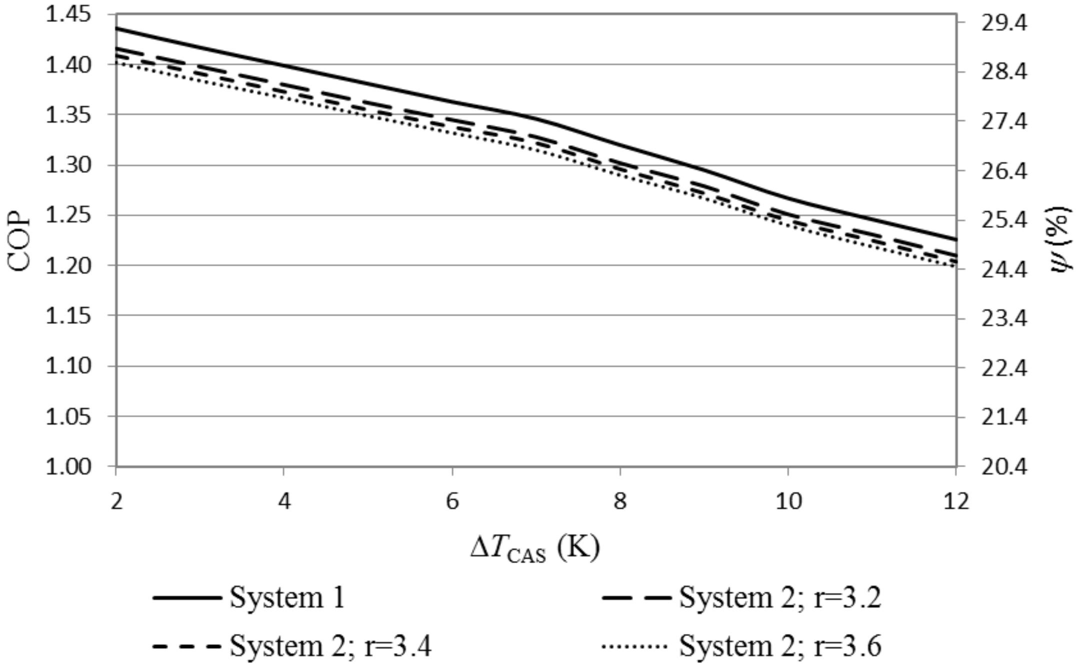


Fig. 7. Variation of system COP and exergy efficiency with cascade heat exchanger temperature difference.

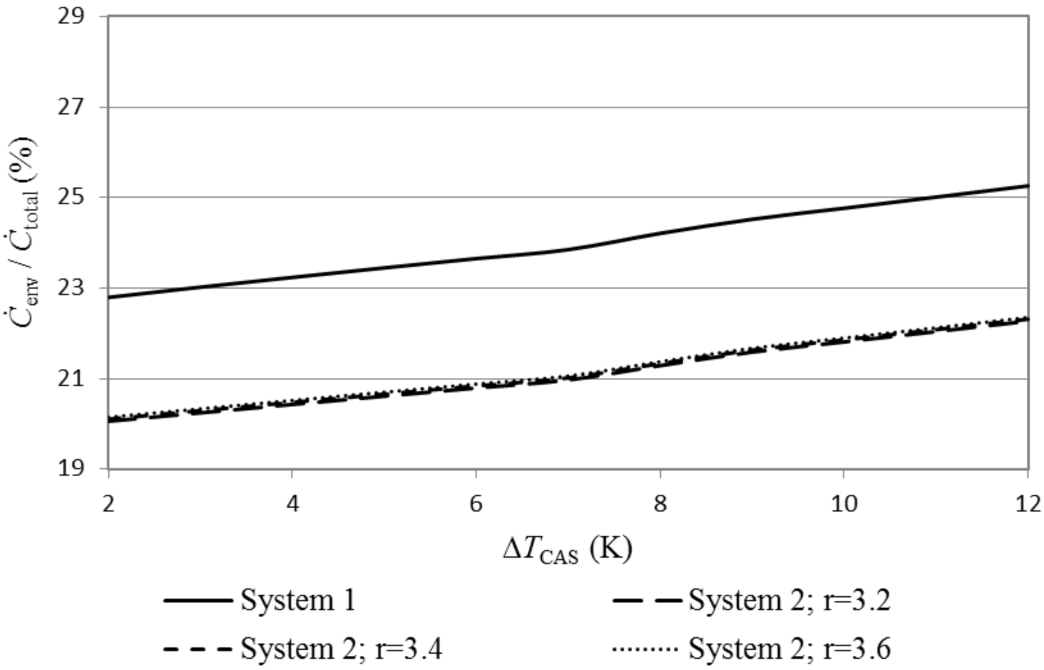


(a)

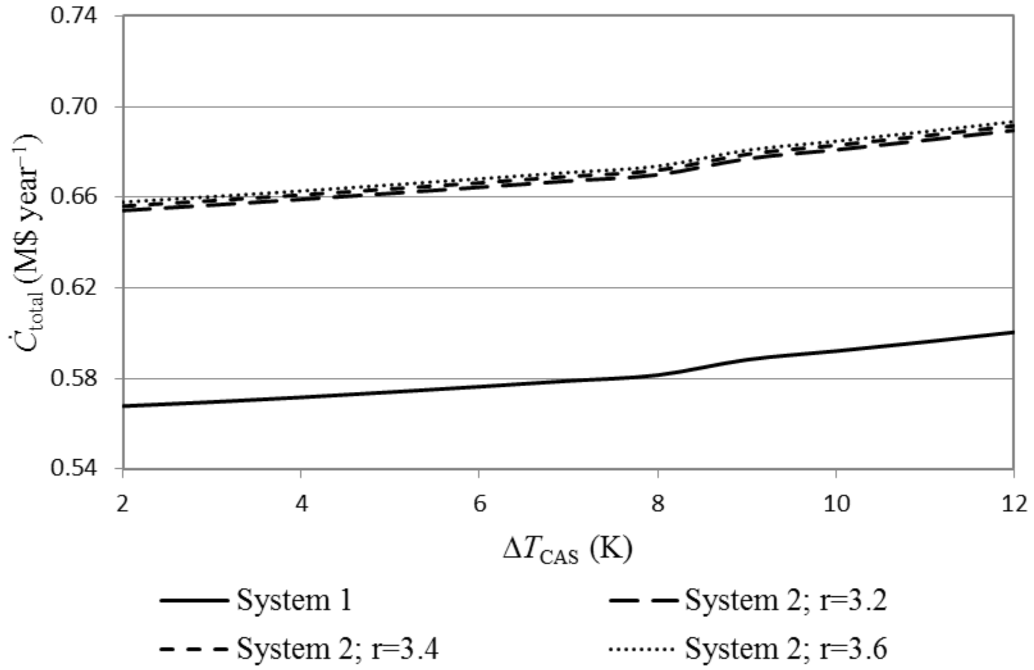


(b)

Fig. 8. Effect of varying cascade heat exchanger temperature difference on (a) the ratio of penalty cost of GHG emission and (b) total annual cost rate.

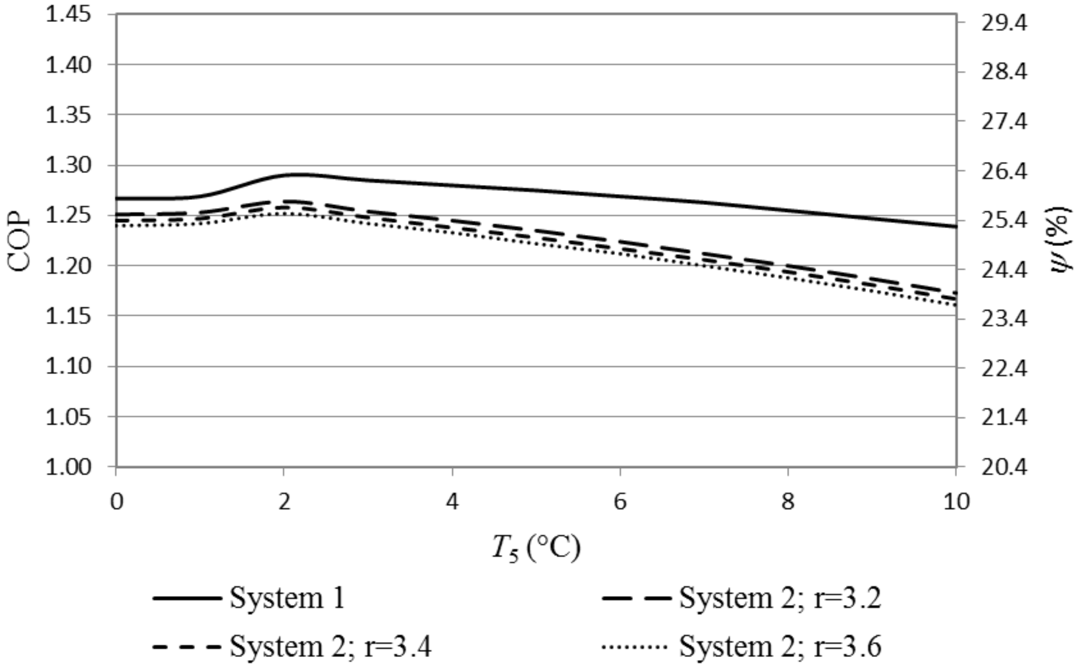


Fig. 9. Variation of system COP and exergy efficiency with $CO_2$ condensing temperature.

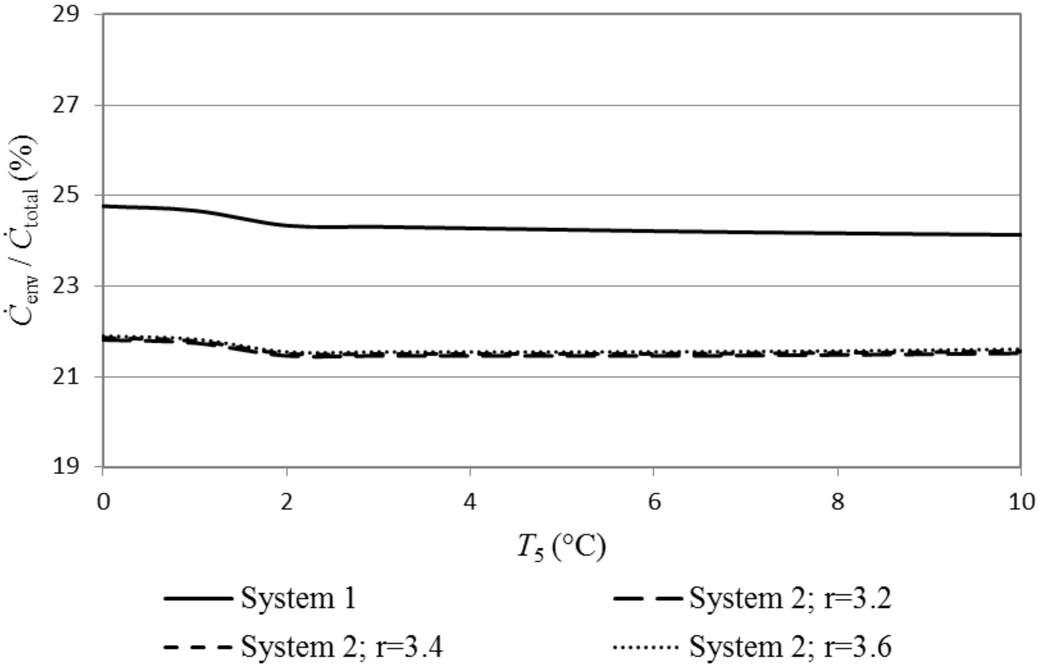


(a)

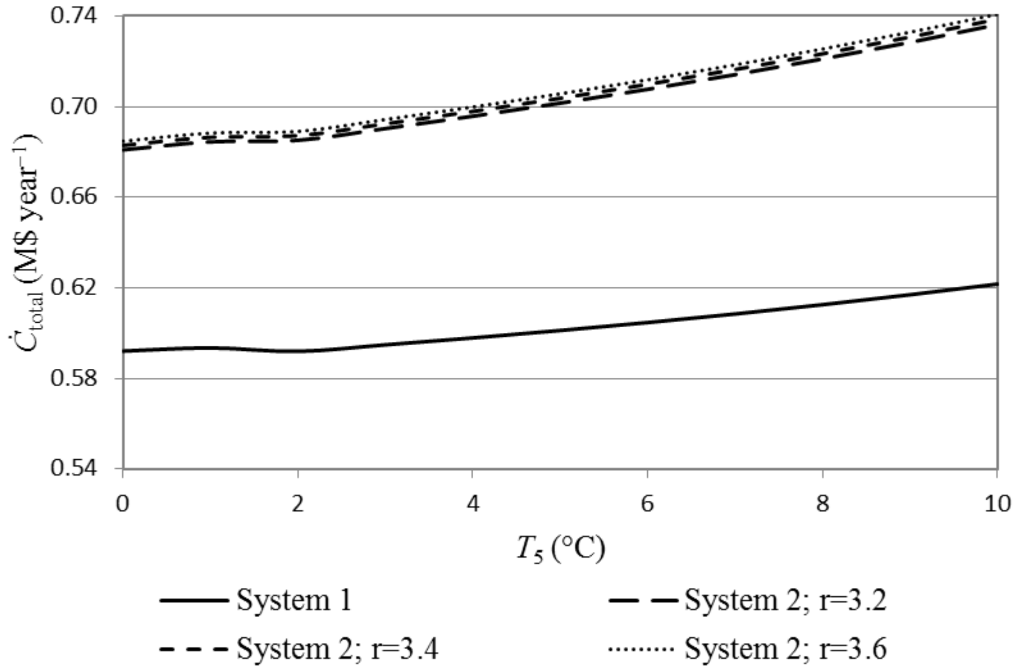


(b)

Fig. 10. Effect of varying $CO_2$ condensing temperature on (a) the ratio of penalty cost of GHG emission and (b) the total annual cost rate.

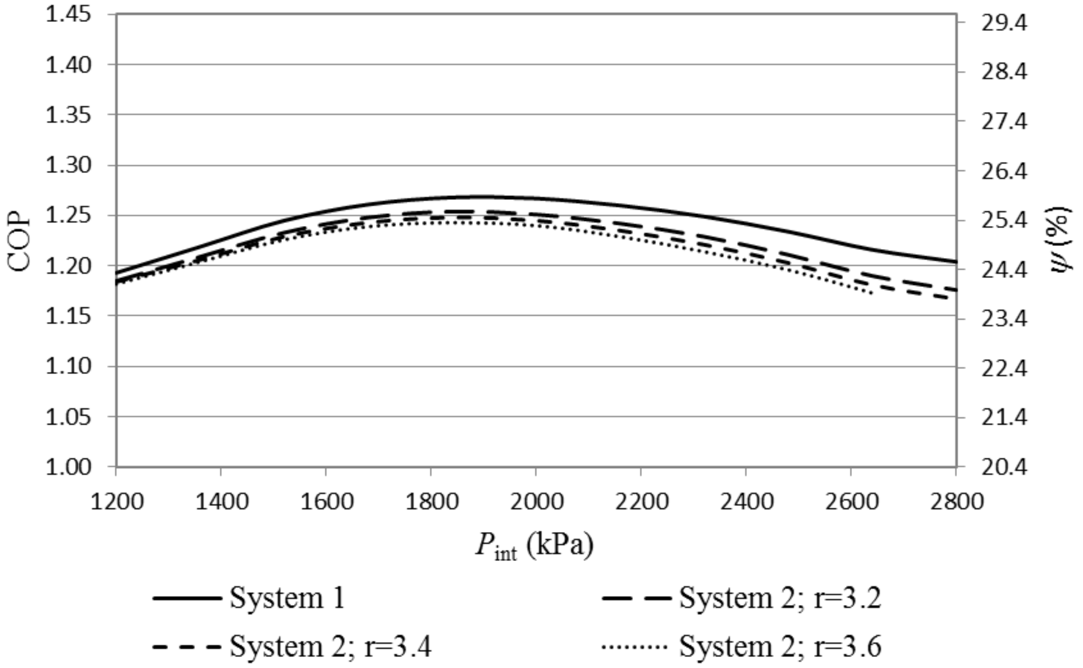


Fig. 11. Variation of system COP and exergy efficiency with intermediate pressure in the low-temperature circuit.

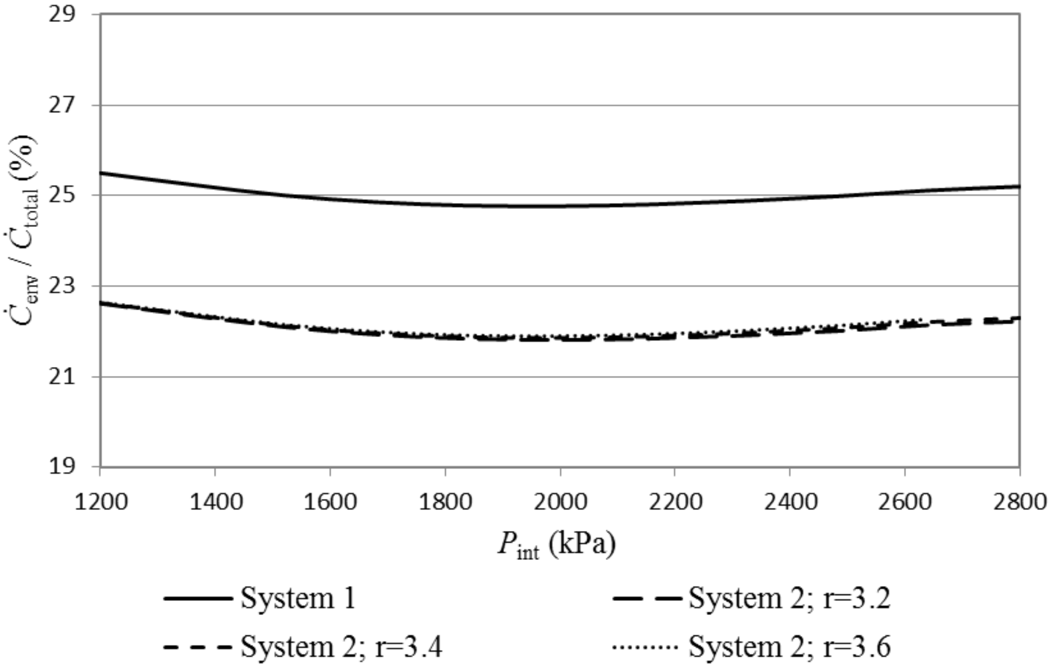


(a)

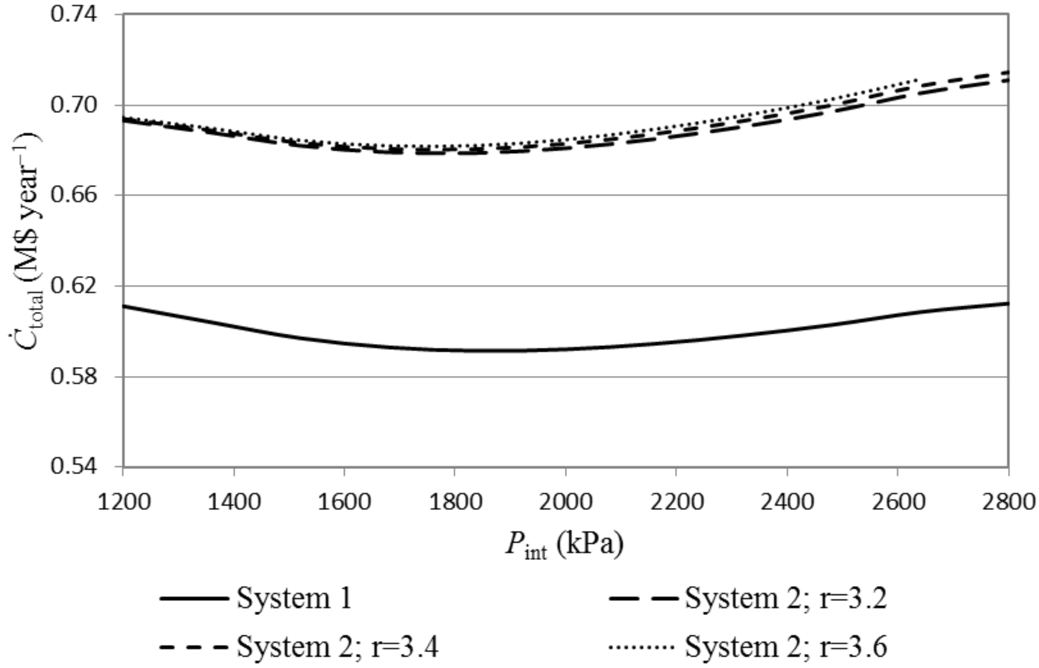


(b)

Fig. 12. Effect of varying intermediate pressure in the low-temperature circuit on (a) the ratio of penalty cost of GHG emission and (b) the total annual cost rate.

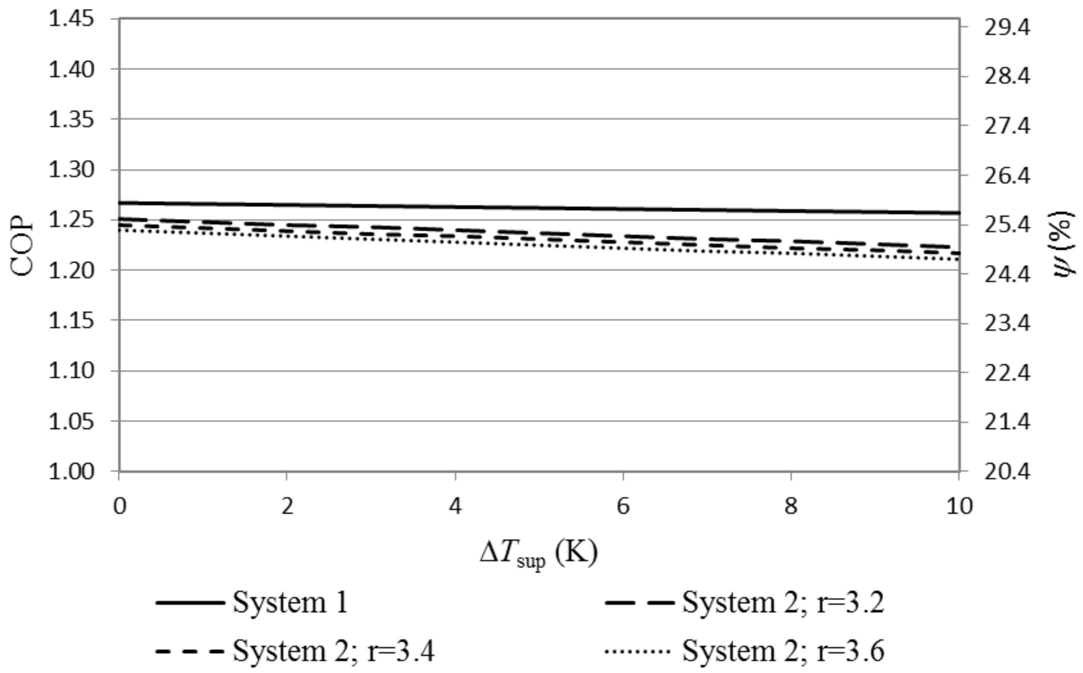


Fig. 13. Variation of systemCOP and exergy efficiency with degree of superheating of $CO_2$ at evaporator outlet.

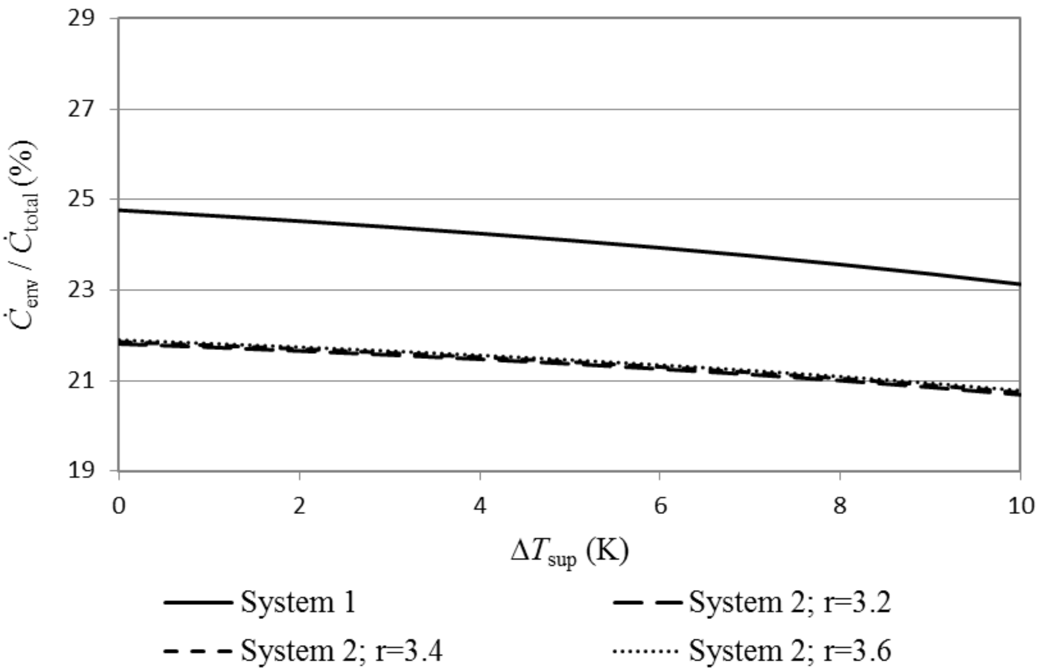


(a)

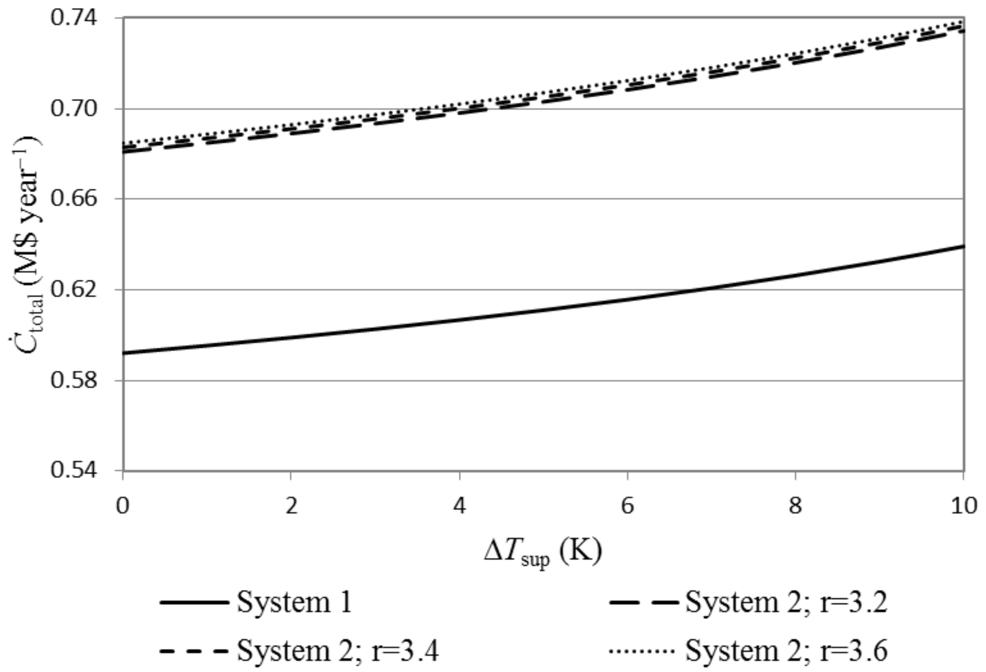


(b)

Fig. 14. Effect of varying superheating degree of $CO_2$ at evaporator outlet on (a) the ratio of penalty cost of GHG emission and (b) the total annual cost rate.

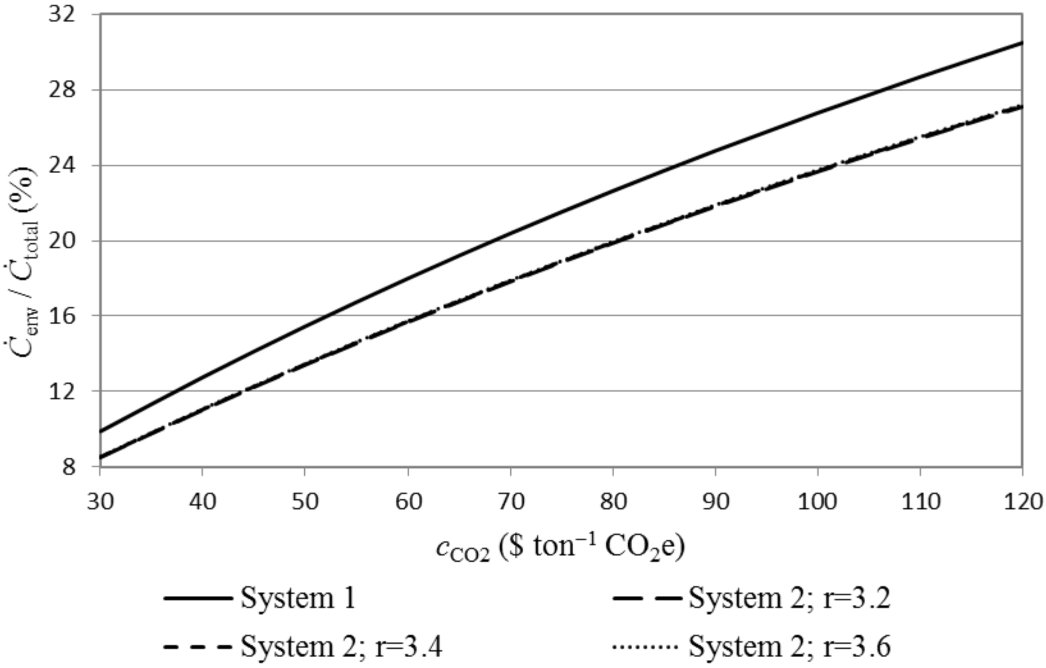


(a)

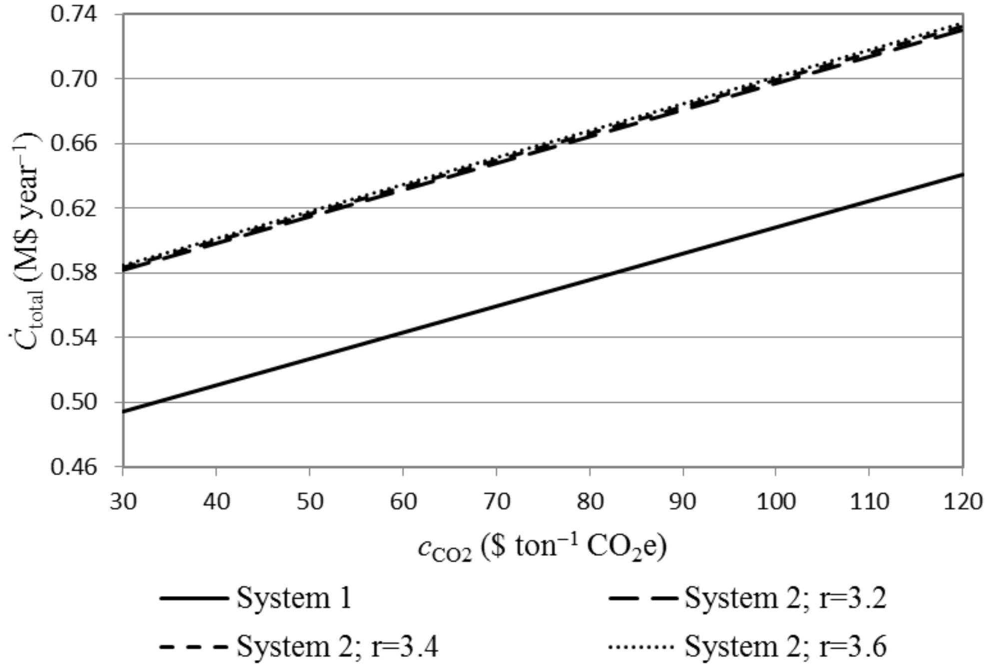


(b)

Fig. 15. Effect of varying cost of $CO_2$ avoided on (a) the ratio of penalty cost of GHG emission and (b) the total annual cost rate.

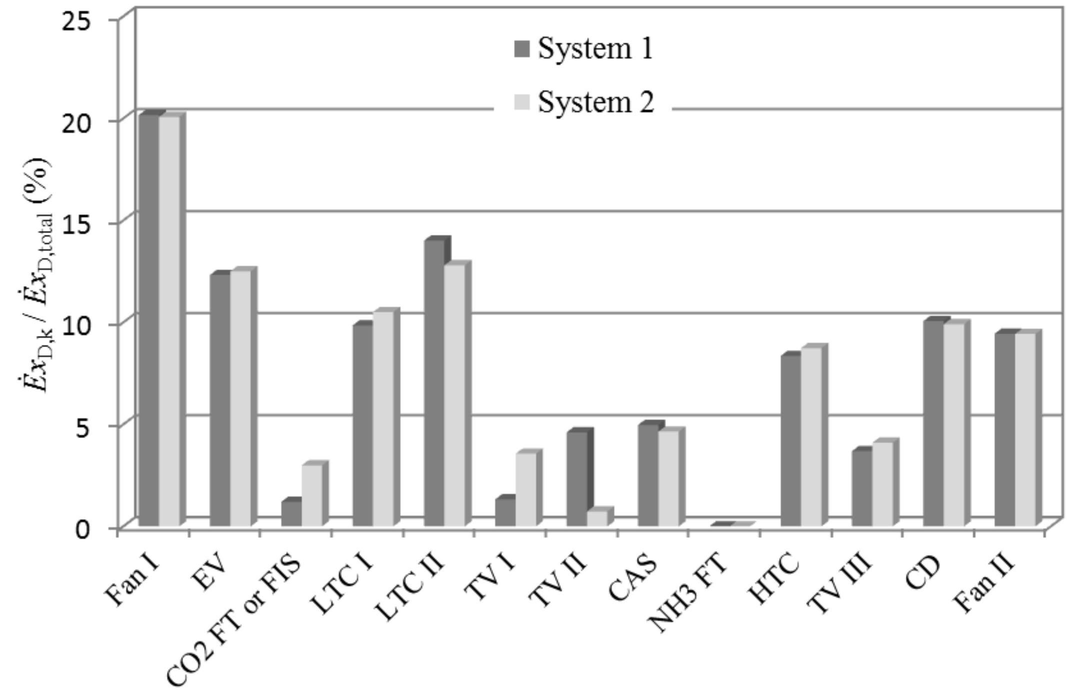


Fig. 16. Relative exergy destruction rate in components of the proposed cascade cycles operating at the thermodynamic optimal design condition.

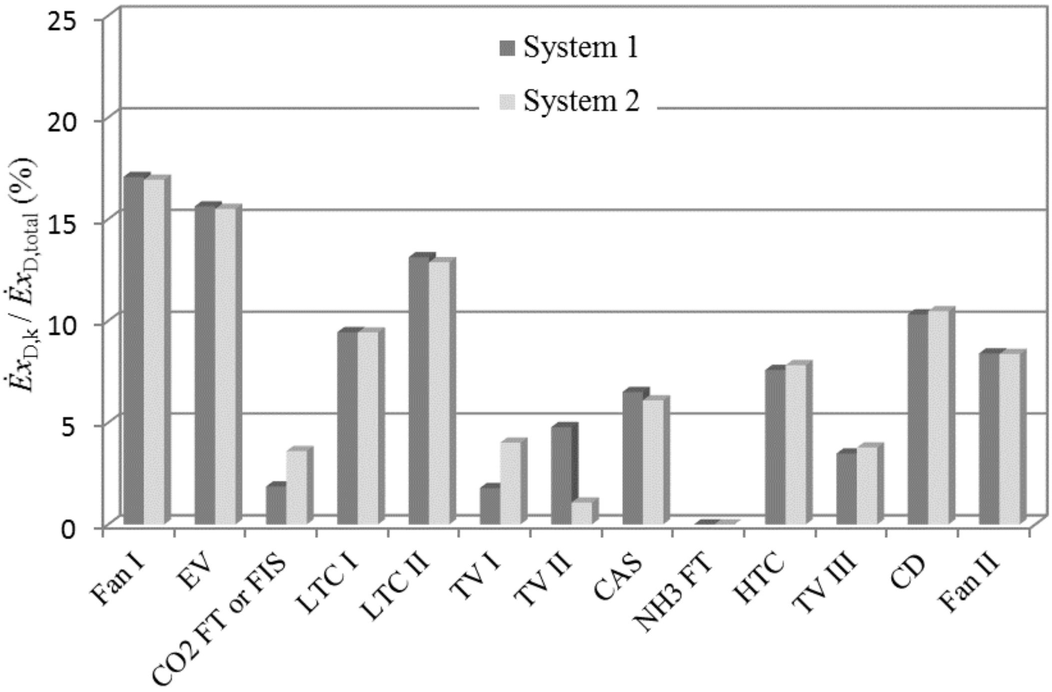


Fig. 17. Relative exergy destruction rates in components of the proposed cascade cycles operating at the cost optimal design condition.

Table 1. Fuel and product exergy rate for various components in two cycles.

| Component | $\dot{E}x_{F}$ | $\dot{E}x_{P}$ |
| --- | --- | --- |
| Fan I | $\dot{W}_{Fan\,I}$ | $\dot{E}x_{ca,i} - \dot{E}x_{ca,i}$ |
| Evaporator | $\dot{E}x_{8} - \dot{E}x_{1}$ | $\dot{E}x_{ca,e} - \dot{E}x_{ca,i'}$ |
| $CO_2$ flash tanks | $\dot{E}x_{6} - \dot{E}x_{7}$ | $\dot{E}x_{3} - \dot{E}x_{2}$ |
| Flash intercooler with indirect subcooler | $\left(\dot{m}_{7}/\dot{m}_{5}\right)\dot{E}x_{5} + \dot{E}x_{6} - \dot{E}x_{7}$ | $\dot{E}x_{3} - \dot{E}x_{2}$ |
| Low-temperature compressor I | $\dot{W}_{LTC\,I}$ | $\dot{E}x_{2} - \dot{E}x_{1}$ |
| Low-temperature compressor II | $\dot{W}_{LTC\,II}$ | $\dot{E}x_{4} - \dot{E}x_{3}$ |
| Throttling valve I | $\dot{E}x_{m,7} - \dot{E}x_{m,8}$ | $\dot{E}x_{t,8} - \dot{E}x_{t,7}$ |
| Throttling valve II | $\dot{E}x_{m,5} - \dot{E}x_{m,6}$ | $\dot{E}x_{t,6} - \dot{E}x_{t,5}$ |
| Cascade heat exchanger | $\dot{E}x_{13} - \left(\dot{m}_{13}/\dot{m}_{9}\right)\dot{E}x_{9}$ | $\dot{E}x_{5} - \dot{E}x_{4}$ |
| $NH_3$ flash tank | $\dot{E}x_{12} - \dot{E}x_{13}$ | $\dot{E}x_{9} - \left(\dot{m}_{13}/\dot{m}_{9}\right)\dot{E}x_{9}$ |
| High-temperature compressor | $\dot{W}_{HTC\,I}$ | $\dot{E}x_{10} - \dot{E}x_{9}$ |
| Throttling valve III | $\dot{E}x_{m,11} - \dot{E}x_{m,12}$ | $\dot{E}x_{t,12} - \dot{E}x_{t,11}$ |
| Condenser | $\dot{E}x_{10} - \dot{E}x_{11}$ | $\dot{E}x_{env,e} - \dot{E}x_{env,i'}$ |
| Fan II | $\dot{W}_{Fan\,II}$ | $\dot{E}x_{env,i'} - \dot{E}x_{env,i}$ |

Table 2. Cost functions of various components [29–32].

| Component | Capital cost function ($Z$) |
|---|---|
| Evaporator and condenser | $1397 \times A_{\mathrm{EV\ or\ CD}}^{0.89}$ |
| Cascade heat exchanger | $383.5 \times A_{\mathrm{CAS}}^{0.65}$ |
| Low-temperature compressor | $10167.5 \times W_{\mathrm{LTC}}^{0.46}$ |
| High-temperature compressor | $9624.2 \times W_{\mathrm{HTC}}^{0.46}$ |
| Flash tank | $280.3 \times \dot{m}_{\mathrm{i}}^{0.67}$ |
| Flash intercooler with indirect subcooler | $1438.1 \times A_{\mathrm{FI}}^{0.65}$ |
| Throttling valve | $114.5 \times \dot{m}$ |
| Fan | $155 \times (\dot{V} + 1.43)$ |
| Installation of refrigeration system | $150.2 \times \dot{Q}_{\mathrm{EV}}$ |

Table 3. Thermodynamic conditions considered in modelling.

| Parameter | Value |
|---|---|
| Cooling capacity, $\dot{Q}_{EV}$ | 500 kW |
| Condensing temperature of $NH_3$, $T_{CD}$ | 35 °C |
| Evaporating temperature of $CO_2$, $T_{EV}$ | –40 °C |
| Degree of superheating of $CO_2$ at evaporator outlet, $\Delta T_{sup}\left(=T_1-T_8\right)$ | 0 K |
| Temperature difference of air in evaporator and condenser | 10 K |
| Condensing temperature of $CO_2$, $T_5$ | 0 °C |
| Cascade heat exchanger temperature difference, $\Delta T_{CAS}\left(=T_5-T_{13}\right)$ | 10 K |
| Temperature of the inlet air to the evaporator, $T_{ca,\,i}$ | –20 °C |
| Ambient temperature, $T_{env,i}$ | 25 °C |
| Ambient pressure, $P_0$ | 101.3 kPa |
| Intermediate pressure of flash tank in $CO_2$ circuit, $P_{int}$ | 2000 kPa |
| Overall heat transfer coefficient of evaporator, $U_{EV}$ | 30 W m$^{-2}$ K$^{-1}$ |
| Overall heat transfer coefficient of condenser, $U_{CD}$ | 40 W m$^{-2}$ K$^{-1}$ |
| Overall heat transfer coefficient of cascade heat exchanger, $U_{CAS}$ | 1000 W m$^{-2}$ K$^{-1}$ |
| Overall heat transfer coefficient of flash intercooler, $U_{FIS}$ | 1000 W m$^{-2}$ K$^{-1}$ |

Table 4. Comparison of performance parameters obtained from present modelling for a basic $CO_2/NH_3$ cascade refrigeration system and the corresponding results reported elsewhere.

| | Operational conditions | | | |
|---|---|---|---|---|
| | $\dot{Q}_{EV} = 40\,kW$, $T_{CD} = 56.3\,°C$, $T_{EV} = -56\,°C$, $T_5 = -8.1\,°C$, $\Delta T_{CAS} = 3.44\,°C$, $N = 6570\,h$ | | $\dot{Q}_{EV} = 50\,kW$, $T_{CD} = 40.1\,°C$, $T_{EV} = -48.7\,°C$, $T_5 = -7.1\,°C$, $\Delta T_{CAS} = 2\,°C$, $N = 7000\,h$ | |
| Parameter | Present work | Ref. [18] | Present work | Ref. [29] |
| $\dot{W}_{total}$ (kW) | 62.96 | 63.01 | 32.57 | 33.44 |
| COP | 0.635 | 0.634 | 1.53 | 1.49 |
| $\psi$ (%) | 19.49 | 19.48 | 47.10 | 45.89 |
| $\dot{C}_f$ ($ year$^{-1}$) | 28,954 | 28,978 | 13,681 | 14,048 |
| $\dot{C}_{total}$ ($ year$^{-1}$) | 110,683 | 109,242 | - | - |

Table 5. Results of thermodynamic optimization for two cycles.

| Parameter | System 1 | System 2 |
|---|---|---|
| $T_{EV}$ (°C) | –35 | –35.20 |
| $T_{CD}$ (°C) | 35 | 35.01 |
| $T_5$ (°C) | 0.01 | –1.98 |
| $\Delta T_{CAS}$ (K) | 2.01 | 2.27 |
| $\Delta T_{sup}$ (K) | 0.10 | 0.45 |
| $P_{int}$ (kPa) | 1861 | 1935 |
| $r$ | - | 3.79 |
| $A_{EV}$ (m$^2$) | 1686 | 1671 |
| $A_{CD}$ (m$^2$) | 659.2 | 627.6 |
| $A_{CAS}$ (m$^2$) | 57.32 | 59.86 |
| $\sum \dot{W}_{CM}$ (kW) | 265.13 | 267.37 |
| $\dot{E}x_{D,total}$ (kW) | 222.5 | 223.5 |
| COP | 1.547 | 1.536 |
| $\psi$ (%) | 31.52 | 31.30 |
| $\dot{C}_{env}$ (\$ year$^{-1}$) | 120,150 | 121,007 |
| $\dot{C}_{total}$ (\$ year$^{-1}$) | 600,006 | 675,530 |

Table 6. Results of cost optimization for two cycles.

| Parameter | System 1 | System 2 |
|---|---|---|
| $T_{EV}$ (°C) | –40 | –40 |
| $T_{CD}$ (°C) | 36.2 | 36.67 |
| $T_5$ (°C) | 1.66 | 0.0 |
| $\Delta T_{CAS}$ (K) | 3.67 | 3.33 |
| $\Delta T_{sup}$ (K) | 1.67 | 1.67 |
| $P_{int}$ (kPa) | 1833 | 1750 |
| $r$ | - | 3.2 |
| $A_{EV}$ ($m^2$) | 1148 | 1148 |
| $A_{CD}$ ($m^2$) | 644.3 | 612.6 |
| $A_{CAS}$ ($m^2$) | 45.61 | 46.81 |
| $\sum \dot{W}_{CM}$ (kW) | 304.19 | 307.93 |
| $\dot{E}x_{D,total}$ (kW) | 262.76 | 264.8 |
| COP | 1.38 | 1.36 |
| $\psi$ (%) | 28.04 | 27.75 |
| $\dot{C}_{env}$ (\$ $year^{-1}$) | 135,082 | 136,494 |
| $\dot{C}_{total}$ (\$ $year^{-1}$) | 580,387 | 661,197 |

Table 7. Exergoeconomic analysis results for the thermodynamic optimal design conditions of the presented systems.

| Component | System 1 | | | System 2 | | |
|---|---|---|---|---|---|---|
| | $\psi_k$ (%) | $c_{F,k}$ (\$ GJ$^{-1}$) | $f_k$ (%) | $\psi_k$ (%) | $c_{F,k}$ (\$ GJ$^{-1}$) | $f_k$ (%) |
| Fan I | 19.62 | 25.0 | 5.46 | 19.62 | 25.0 | 5.46 |
| Evaporator | 79.96 | 174.5 | 70.95 | 79.63 | 502.2 | 45.03 |
| $CO_2$ flash tank | 97.48 | 172.6 | 1.73 | - | - | - |
| Flash intercooler with liquid subcooler | - | - | - | 93.29 | 504.2 | 63.70 |
| Low-temperature compressor I | 56.53 | 25.0 | 55.83 | 59.07 | 25.0 | 55.57 |
| Low-temperature compressor II | 65.53 | 25.0 | 53.80 | 63.12 | 25.0 | 54.18 |
| Throttling valve I | 92.64 | 172.6 | 30.43 | 91.62 | 495.8 | 5.60 |
| Throttling valve II | 85.82 | 168.6 | 14.74 | 87.20 | 495.8 | 7.07 |
| Cascade heat exchanger | 85.43 | 155.5 | 19.46 | 87.21 | 148.3 | 3.85 |
| $NH_3$ flash tank | 100 | 155.5 | 100 | 100 | 148.3 | 100 |
| High-temperature compressor | 85.04 | 25.0 | 68.14 | 85.30 | 25.0 | 67.74 |
| Throttling valve III | 90.54 | 145.5 | 38.72 | 90.17 | 137.8 | 37.27 |
| Condenser | 3.76 | 114.0 | 66.52 | 3.54 | 107.2 | 67.15 |
| Fan II | 1.67 | 25.0 | 17.91 | 1.67 | 25.0 | 17.91 |

Table 8. Exergoeconomic analysis results for the cost optimal design conditions of the presented systems.

| | System 1 | | | System 2 | | |
|---|---|---|---|---|---|---|
| Component | $\psi_k$ (%) | $c_{F,k}$ (\$ GJ$^{-1}$) | $f_k$ (%) | $\psi_k$ (%) | $c_{F,k}$ (\$ GJ$^{-1}$) | $f_k$ (%) |
| Fan I | 19.62 | 25.0 | 5.46 | 19.62 | 25.0 | 5.46 |
| Evaporator | 72.68 | 188.9 | 51.81 | 72.68 | 485.9 | 29.83 |
| $CO_2$ flash tank | 96.22 | 186.1 | 1.89 | - | - | - |
| Flash intercooler with liquid subcooler | - | - | - | 91.50 | 484.3 | 55.82 |
| Low-temperature compressor I | 62.61 | 25.0 | 55.91 | 61.21 | 25.0 | 55.41 |
| Low-temperature compressor II | 66.58 | 25.0 | 52.79 | 66.44 | 25.0 | 52.89 |
| Throttling valve I | 91.61 | 186.1 | 20.48 | 90.84 | 472.7 | 4.44 |
| Throttling valve II | 84.78 | 181.2 | 12.14 | 85.36 | 472.7 | 5.14 |
| Cascade heat exchanger | 78.43 | 155.3 | 12.00 | 80.43 | 108.1 | 2.12 |
| $NH_3$ flash tank | 100 | 155.3 | 100 | 100 | 150.0 | 100 |
| High-temperature compressor | 85.19 | 25.0 | 67.41 | 85.39 | 25.0 | 67.10 |
| Throttling valve III | 89.95 | 143.7 | 37.54 | 89.51 | 139.3 | 36.19 |
| Condenser | 3.25 | 110.3 | 61.98 | 2.99 | 108.1 | 61.28 |
| Fan II | 1.66 | 25.0 | 17.89 | 1.66 | 25.0 | 17.89 |